

# Weighted Sub-fractional Brownian Motion Process: Properties and Generalizations.

J.H. Ramírez-González, Ying Sun

<sup>a</sup>King Abdullah University Of Science And Technology, Thuwal, 23955, Makkah, Saudi Arabia

---

## Abstract

In this paper, we present several path properties, simulations, inferences, and generalizations of the weighted sub-fractional Brownian motion. A primary focus is on the derivation of the covariance function  $R_{f,b}(s, t)$  for the weighted sub-fractional Brownian motion, defined as:

$$R_{f,b}(s, t) = \frac{1}{1-b} \int_0^{s \wedge t} f(r) [(s-r)^b + (t-r)^b - (t+s-2r)^b] dr,$$

where  $f : \mathbb{R}_+ \rightarrow \mathbb{R}_+$  is a measurable function and  $b \in [0, 1) \cup (1, 2]$ . This covariance function  $R_{f,b}(s, t)$  is used to define the centered Gaussian process  $\zeta_{t,f,b}$ , which is the weighted sub-fractional Brownian motion. Furthermore, if there is a positive constant  $c$  and  $a \in (-1, \infty)$  such that  $0 \leq f(u) \leq cu^a$  on  $[0, T]$  for some  $T > 0$ . Then, for  $b \in (0, 1)$ ,  $\zeta_{t,f,b}$  exhibits infinite variation and zero quadratic variation, making it a non-semi-martingale. On the other hand, for  $b \in (1, 2]$ ,  $\zeta_{t,f,b}$  is a continuous process of finite variation and thus a semi-martingale and for  $b = 0$  the process  $\zeta_{t,f,0}$  is a square-integrable continuous martingale. We also provide inferential studies using maximum likelihood estimation and perform simulations comparing various numerical methods for their efficiency in computing the finite-dimensional distributions of  $\zeta_{t,f,b}$ . Additionally, we extend the weighted sub-fractional Brownian motion to  $\mathbb{R}^d$  by defining new covariance structures for measurable, bounded sets in  $\mathbb{R}^d$ . Finally, we define a stochastic integral with respect to  $\zeta_{t,f,b}$  and introduce both the weighted sub-fractional Ornstein-Uhlenbeck process and the geometric weighted sub-fractional Brownian motion.

**Keywords:** branching particle systems, Gaussian processes, geometric process, long memory processes, Ornstein–Uhlenbeck process, weighted processes.

**2020 MSC:** subject classifications: 60G15.

---

## 1. Introduction

In this paper, we present several path properties, simulations, inferences and generalizations of the weighted sub-fractional Brownian motion. We start by providing a historical context and background on the development of this family of Gaussian processes. Vatutin and Wakolbinger (1998) and Fleischmann et al. (2002) investigated the  $(d, \alpha, \theta, \gamma)$ -branching particle system, characterized as a non-Markovian  $(1 + \theta)$ -branching particle system. This system originates from a Poissonian population with intensity measure  $\Lambda$ , where particles move on  $\mathbb{R}^d$  according to an  $\alpha$ -stable motion with index  $\alpha \in (0, 2]$ , and their lifetimes follow a common distribution function  $F$ . The authors examined two scenarios: when  $F$  has a finite mean, and when  $F$  belongs to the domain of attraction of a  $\gamma$ -stable law with  $0 < \gamma < 1$ , specifically  $1 - F(t) \sim c_\gamma t^{-\gamma}$  as  $t \rightarrow \infty$ , for some positive constant  $c_\gamma$ . They demonstrated that the system remains persistent if and only if  $d \geq a\gamma/\theta$  and  $d > a/\theta$  in the case of lifetimes with a finite mean, which includes the Markovian case where lifetimes distribution follow an exponential distribution. Specifically, suppose the system starts with a particle at position  $x \in \mathbb{R}^d$ ,  $d \in \mathbb{N}$ . The particle lives for a random time  $\tau$  with distribution function  $F$ , during which it moves on  $\mathbb{R}^d$  according to an  $\alpha$ -stable spherically symmetric motion. At the end of its lifetime, it gives rise to a random number  $\xi$  of offspring particles. The offspring distribution follows the so-called  $(1 + \theta)$ -distribution,  $0 < \theta \leq 1$ , characterized by the probability generating function  $f(s) = s + c(1 - s)^{1+\theta}$ ,  $0 \leq s \leq 1$ , where  $c \in (0, 1/(1 + \theta)]$ . In particular, for  $\theta = 1$  and  $c = 1/2$  we have critical binary branching. Each offspring particle then follows the same dynamics as the original, subject to the usual assumption of independence.

Let  $Z(t)$  be the counting measure in  $\mathbb{R}^d$  representing the positions of particles alive at time  $t$ . The occupation time of  $Z$ , denoted by  $J \equiv \{J(t), t \geq 0\}$ , is given by:

$$\langle \varphi, J(t) \rangle = \int_0^t \langle \varphi, Z(s) \rangle ds,$$

for bounded measurable functions  $\varphi : \mathbb{R}^d \rightarrow \mathbb{R}_+$ . The rescaled occupation time process  $J_T(t) = J(Tt)$  and the fluctuation process  $\mathcal{J}_T(t)$  defined by:

$$\langle \varphi, \mathcal{J}_T(t) \rangle = \frac{1}{H_T} (\langle \varphi, J_T(t) \rangle - Tt \langle \varphi, \Lambda \rangle),$$

where  $H_T$  is a normalization factor.

Under critical binary branching assumption, Bojdecki et al. (2004b) demonstrated that for exponentially distributed lifetimes and dimensions satisfying  $\alpha <$

$d < 2\alpha$ , the rescaled occupation time fluctuation process converges weakly toward a Gaussian process in the space  $C([0, \eta], \mathcal{S}')$  of continuous paths  $w : [0, \eta] \rightarrow \mathcal{S}'$  for any  $\eta > 0$ , where  $\mathcal{S}'$  denotes the space of tempered distributions, i.e., the strong dual of the space  $\mathcal{S}$  of rapidly decreasing smooth functions. The limit process has a simple spatial structure, whereas the temporal structure is characterized by a Gaussian process  $\eta = \{\eta_t, t \geq 0\}$  with covariance function

$$\mathbb{E}(\eta_s \eta_t) := C_h(s, t) = (2 - h) \left( s^h + t^h - \frac{1}{2} \left[ (s + t)^h + |s - t|^h \right] \right), \quad s, t \geq 0,$$

where  $h = 3 - d/\alpha$  and  $h \in (1, 2)$ . Later, (López-Mimbela et al., 2024, Thm. 2.2) showed that the same result is satisfied when the particle lifetimes have a distribution with finite mean. In Bojdecki et al. (2007), the authors showed that  $C_h(s, t)$  is a covariance function if and only if  $0 < h \leq 4$ . In the case  $0 < h \leq 2$ ,  $\{\eta_t, t \geq 0\}$  is called sub-fractional Brownian motion and has the representation:

$$\eta_t = \frac{1}{\sqrt{2}} (\epsilon_t + \epsilon_{-t}),$$

where  $\epsilon$  is a fractional Brownian motion (fBm) defined for all  $-\infty < t < \infty$ . When  $2 < h \leq 4$ ,  $\eta = \{\eta_t, t \geq 0\}$  is called negative sub-fractional Brownian motion and has the representation:

$$\left( \frac{1}{2} h(h-1)(h-2) \right)^{1/2} \int_0^t v_s ds,$$

where  $v$  is a centered continuous Gaussian process with covariance

$$(s + t)^{h-2} - |s - t|^{h-2}.$$

In Bojdecki et al. (2008), the authors investigated the limit fluctuations of a rescaled occupation time process of a branching particle system with particles moving according to  $d$ -dimensional  $\alpha$ -stable motion, starting with an inhomogeneous Poisson population with intensity measure  $\frac{dx}{1+|x|^\gamma}$ , where  $\gamma > 0$ . In this case, for  $\gamma < d < \alpha$  and normalization  $T^{1-(d+\gamma)/2\alpha}$ , the limit of the occupation time fluctuations is a Gaussian process whose temporal structure is determined by the covariance function:

$$C_{a,b}(w, z) := \int_0^{z \wedge w} s^a [(z - s)^b + (w - s)^b] ds, \quad w, z \geq 0, \quad (1)$$

for  $a = -\gamma/\alpha$  and  $b = 1 - d/\alpha$ . In Bojdecki et al. (2007), it was shown that the maximum range of values of the parameters  $a, b$  for which (1) is a function of covariance. They proved that  $C_{a,b}$  is a covariance function if and only if  $a > -1$ ,  $-1 < b \leq 1$ , and  $|b| \leq 1 + a$ . The authors named the centered Gaussian process with the covariance function (1) as *weighted fractional Brownian motion with parameters  $a$  and  $b$* . This designation is justified because when  $a = 0$ , the covariance function simplifies to:

$$C_{0,b}(s, t) = \frac{1}{b+1} \left( t^{b+1} + s^{b+1} - |s-t|^{b+1} \right),$$

which corresponds to the covariance function of a fractional Brownian motion with Hurst parameter  $\frac{1}{2}(b+1)$ . In Litan Yan et al. (2014), various properties of the weighted fractional Brownian motion were studied, such as the law of the iterated logarithm,  $\alpha$ -variation, etc.

Along the same line of research, López-Mimbela et al. (2024) investigated the occupation time fluctuations of the  $(d, \alpha, \theta, \gamma)$ -branching particle system with critical binary branching. Under assumption of  $F$  belonging to the domain of attraction of a  $\gamma$ -stable law with  $0 < \gamma < 1$ . The authors proved that for  $\alpha\gamma < d < \alpha(1 + \gamma)$ , the temporal structure of the mentioned fluctuations is dictated by a centered Gaussian process with covariance structure: for  $d \neq \alpha$  and  $s, t \geq 0$ ,

$$Q(s, t) = \left( \frac{d}{\alpha} - 1 \right)^{-1} \int_0^{s \wedge t} r^{\gamma-1} \left[ (s-r)^{2-d/\alpha} + (t-r)^{2-d/\alpha} - (t+s-2r)^{2-d/\alpha} \right] dr,$$

and in the critical case  $d = \alpha$ , by:

$$K(s, t) = \int_0^{s \wedge t} r^{\gamma-1} [(s+t-2r) \ln(s+t-2r) - (s-r) \ln(s-r) - (t-r) \ln(t-r)] dr. \quad (2)$$

Furthermore, considering  $a = \gamma - 1 \in (-1, 0)$  and  $b = 2 - \frac{d}{\alpha} \in (1, 2)$ , they introduced a generalization of the covariance function  $Q(s, t)$  and called the corresponding Gaussian process *weighted sub-fractional Brownian motion*. For  $a, b > -1$  with  $b \neq 1$ , the function

$$Q_{a,b}(w, z) := \frac{1}{1-b} \int_0^{z \wedge w} s^a \left[ (z-s)^b + (w-s)^b - (w+z-2s)^b \right] ds, \quad w, z \geq 0, \quad (3)$$

is positive definite in the following cases: (i)  $a > -1$  and  $0 \leq b \leq 2$ ; (ii)  $a > -1$  and  $-1 < b < 0$  with  $a + b + 1 \geq 0$ . However, the function  $Q_{a,b}(s, t)$  is not a covariance function in the following cases: (i)  $a > -1$  and  $-1 < b < 0$  with

$a + b + 1 < 0$ ; (ii)  $a > -1$  and  $b > a + 3$ . They could not determine whether (3) is positive definite for  $a > -1$  and  $2 < b \leq a + 3$ , which remains an open problem. When  $a = 0$ ,

$$Q_{0,b}(w, z) = \frac{1}{(b+1)(1-b)} \left( w^{b+1} + z^{b+1} - \frac{1}{2} \left( (w+z)^{b+1} + |w-z|^{b+1} \right) \right), \quad w, z \geq 0. \quad (4)$$

Therefore, (3) coincides with the covariance function  $C_h(s, t)$  with  $h = b + 1 \in (0, 4]$ .

Subsequently, Ramírez-González et al. (2024b) presented a more general form of the covariance function (2). Specifically, they considered

$$K_f(s, t) := \int_0^{s \wedge t} f(r) \left[ (s+t-2r) \log(s+t-2r) - (s-r) \log(s-r) - (t-r) \log(t-r) \right] dr, \quad (5)$$

where  $f : \mathbb{R}_+ \rightarrow \mathbb{R}_+$  is a measurable function such that, for any  $\delta > 0$ ,

$$\int_0^\delta f(u) du < \infty. \quad (6)$$

They proved that, under the assumption (6),  $K_f(s, t)$  is a covariance function. We denote by  $\zeta_f = \{\zeta_{t,f}, t \geq 0\}$  the centered Gaussian process with covariance function (5). The authors examined several path and memory properties of the process  $\zeta_f$ , including its variation, quadratic variation, long-range memory, and dependence.

The first goal of this paper is to study a more general form of the covariance function (3) in case  $b \in [0, 1) \cup (1, 2]$ . In Section 2.1, we prove that

$$R_{f,b}(s, t) := \frac{1}{1-b} \int_0^{s \wedge t} f(r) \left[ (s-r)^b + (t-r)^b - (t+s-2r)^b \right] dr, \quad s, t \geq 0, \quad (7)$$

is a covariance function, where  $f : \mathbb{R}_+ \rightarrow \mathbb{R}_+$  is a measurable function such that, for any  $t > 0$ ,

$$\int_0^t f(u)(t-u)^b du < \infty. \quad (8)$$

We restrict to the case of  $b \in [0, 1) \cup (1, 2]$  as for the remaining cases, additional conditions to the integrability condition (8) may be necessary, as mentioned previously for  $f(u) = u^\alpha$  for  $\alpha \in (-1, \infty)$ . When  $f(u) = u^\alpha$ , various properties such

as Hölder continuity, self-similarity, long-range dependence, etc., were studied in López-Mimbela et al. (2024). We denote by  $\zeta_{f,b} = \{\zeta_{t,f,b}, t \geq 0\}$  the centered Gaussian process with covariance function (7). In Section 2.2, we present several path and memory properties of the process  $\zeta_{t,f,b}$ , including long-range memory, long-range dependence, short memory, etc. Additionally, given  $f, g$  positive real-valued functions we write  $f \asymp g$  if there are positive constants  $c_1$  and  $c_2$  such that  $c_1 f \leq g \leq c_2 f$ . Observe that, if  $f \asymp g$  with  $c_1$  and  $c_2$ , then  $g \asymp f$  with  $c_2^{-1}$  and  $c_1^{-1}$ . We suppose that  $1 \asymp f$  or  $u^\alpha \asymp f$  with  $\alpha \in (-1, \infty)$  on  $[0, T]$  for some  $T > 0$ . When  $b \in [0, 1)$ , we show that  $\{\zeta_{t,f,b}, t \geq 0\}$  has infinite variation and quadratic variation equal to 0 almost surely. In particular,  $\{\zeta_{t,f,b}, t \geq 0\}$  is not a semi-martingale. We can define a form of integration with respect to  $\{\zeta_{t,f,b}, t \geq 0\}$  using the approach developed by Russo and Vallois (2000), where a stochastic integration framework for processes with finite quadratic variation is established. In the case  $b \in (1, 2]$ , if there is a positive constant  $c$  and  $a \in (-1, \infty)$  such that  $0 \leq f(u) \leq cu^a$  on  $[0, T]$  for some  $T > 0$ . Then,  $\{\zeta_{t,f,b}, t \geq 0\}$  is a continuous process of finite variation and, therefore, is a semi-martingale. Furthermore, the process  $\{\zeta_{t,f,b}, t \geq 0\}$  has the following integral representation:

$$\zeta_{t,f,b} = \sqrt{b} \int_0^t v_{s,f,b} ds, \quad t \in [0, T] \quad (9)$$

where  $(v_{t,f,b})_{t \geq 0}$  is a Gaussian process with covariance function

$$C_{f,b}(s, t) := \int_0^{s \wedge t} f(u)(s + t - 2u)^{b-2} du$$

Moreover, when  $a \geq 0$  the process  $(\zeta_{t,f,b})_{t \geq 0}$  is a continuously differentiable process with

$$\frac{d\zeta_{t,f,b}}{dt} = \sqrt{b} v_{t,f,b}$$

Finally, under the assumption (6), we prove the following continuity result on the family of covariance functions  $R_{f,b}(s, t)$ :

$$R_{f,b}(s, t) \xrightarrow{b \rightarrow 1} K_f(s, t), \quad \forall s, t \geq 0.$$

In Section 5.1 of supplementary material, we compare different numerical integration methods to optimize the computation time for the finite-dimensional distributions of the process  $\zeta_{t,f,b}$ . We implemented four methods using the R

programming language: Gauss-Kronrod quadrature with Wynn's Epsilon Algorithm, h-adaptive integration, p-adaptive integration, and an approach using known functions to express the integral. Each method's performance was evaluated based on accuracy and computational efficiency. In Section 5.2 of supplementary material, considering the families of functions  $C_1 := \{f_a(u) := u^a \mid u > 0, a > -1\}$  and  $C_2 := \{f_a(u) := e^{au} \mid u > 0, a \in \mathbb{R}\}$ , which satisfy condition (6), we present inferential studies of the finite-dimensional distributions of the process  $\zeta_{t,f,b}$  over  $C_1 \cup C_2$ . Inference was conducted via maximum likelihood estimation using the R software, with the code accessible at <https://github.com/joseramirezgonzalez/Weighted-sfBm>.

In Section 2.3, we extend the weighted sub-fractional Brownian motion to  $\mathbb{R}^d$ . We consider a non-empty, measurable, and bounded set  $A \subset \mathbb{R}^d$  and define  $A_x := \inf\{\|u - x\| \mid u \in A\}$ , where  $\|\cdot\|$  denotes the Euclidean norm on  $\mathbb{R}^d$ . Let  $H \in (0, 1]$  and  $f : \mathbb{R}^d \rightarrow \mathbb{R}_+$  be a function such that for all  $x \in \mathbb{R}^d$ , the following condition is satisfied:

$$\int_{\{u \in \mathbb{R}^d \mid 0 < A_u \leq A_x\}} f(u) \|x - u\|^{2H} du < \infty. \quad (10)$$

We define the covariance functions  $Q_{H,-}(x, y)$  and  $Q_{H,+}(x, y)$  as follows:

$$\begin{aligned} Q_{H,-}(x, y) &:= \|x\|^{2H} + \|y\|^{2H} - \|x - y\|^{2H}, \\ Q_{H,+}(x, y) &:= \|x\|^{2H} + \|y\|^{2H} - \|x + y\|^{2H}. \end{aligned}$$

Both  $Q_{H,+}(x, y)$  and  $Q_{H,-}(x, y)$  are known to be valid covariance functions. Therefore, an extension for  $R_{f,b}$  in the  $d$ -dimensional case involves the following covariance structures:

$$K_{H,A,f,-}(x, y) := \int_{\{u \in \mathbb{R}^d \mid 0 < A_u \leq A_x \wedge A_y\}} f(u) Q_{H,-}(x - u, y - u) du, \quad (11)$$

$$K_{H,A,f,+}(x, y) := \int_{\{u \in \mathbb{R}^d \mid 0 < A_u \leq A_x \wedge A_y\}} f(u) Q_{H,+}(x - u, y - u) du. \quad (12)$$

The covariance function (12) corresponds to  $R_{f,b}$  when considering the space  $\mathbb{R}_+$  instead of  $\mathbb{R}^d$ , with  $A = \{0\}$  and  $b = 2H$  for  $H \in (0, \frac{1}{2})$ . Additionally, we present some extensions by replacing  $Q_{H,+}$  or  $Q_{H,-}$  with stationary covariance functions.

In Section 3, we present the definition and simulations of processes associated with the process  $\zeta_{t,f,b}$ . In Section 3.1, we define the weighted sub-fractional Ornstein-Uhlenbeck process as the solution of the following SDE:

$$dV_{f,b,t} = -\beta V_{f,b,t} dt + \sigma d\zeta_{t,f,b}, \quad \beta \in (-\infty, \infty), \sigma > 0, \quad t \in [0, T]. \quad (13)$$

When  $b \in (1, 2]$ ,  $\zeta_{t,f,b}$  is continuous and of finite variation. Thus, we can use an Itô-type formula to define the weighted sub-fractional Ornstein–Uhlenbeck process. For  $b \in (0, 1)$ , we define the weighted sub-fractional Ornstein–Uhlenbeck process via the forward integral.

The Ornstein–Uhlenbeck (OU) process finds numerous applications across diverse fields, including finance, physics, biology, ecology, and environmental sciences. For example, in finance, the OU process is employed to investigate optimal strategies for investment and reinsurance (Liang et al., 2011). In biological research, the OU process aids in the study of phenotypic trait evolution, taking into account factors such as adaptation and migration (Bartoszek et al., 2017). In the field of ecology, it is commonly used to model animal movement, where each velocity component is represented as an OU process (Johnson et al., 2008). The fractional Ornstein–Uhlenbeck (fOU) process, introduced by Cheridito et al. (2003), extends the traditional OU process by incorporating memory effects of long-range. Ramírez-González and Sun (2023) proposed a model for animal movement where each velocity component along the coordinate axes is treated independently and modeled by a fractional Ornstein–Uhlenbeck (fOU) process. Subsequently, Ramírez-González et al. (2024a) presented a multi-dimensional extension of this model for applications in animal telemetry studies.

In Section 3.2, for  $b \in [0, 1) \cup (1, 2]$ , by integral representation (9), we can define the geometric weighted sub-fractional Brownian motion process  $S_{t,f,b}$  as the solution to the following stochastic differential equation (SDE):

$$dS_{t,f,b} = \mu S_{t,f,b} dt + \sigma S_{t,f,b} d\zeta_{t,f,b}, \quad \mu \in (-\infty, \infty), \sigma > 0, \quad t \in [0, T]. \quad (14)$$

where  $\mu$  is the “percent drift” and  $\sigma$  is the “percent volatility”. The geometric process associated with Gaussian noise has been extensively used in financial modeling due to its ability to capture the stochastic behavior of asset prices. The flexibility of measurable functions  $f : \mathbb{R}_+ \rightarrow \mathbb{R}_+$  that satisfy the integrability condition (8) makes the process  $S_{t,f,b}$  be robust for various applications in finance. For instance, geometric Brownian motion (gBm) has been widely used in financial analysis, particularly in option pricing and risk management, due to its ability to model asset price dynamics effectively. This allows for the derivation of option price equations and provides insights into market behaviors and risk assessment. Cheung et al. (1993) discusses the importance of gBm, presenting a solution to Kolmogorov’s backward equation for gBm and highlighting its applications in finance. Stojkoski et al. (2020) explores the limitations of classical gBm in capturing real asset price dynamics and introduces a generalized geometric Brownian motion (ggBm) with



a memory kernel to address these issues. It presents a comprehensive analysis of moments, log-moments, and probability density functions, demonstrating how ggBm can mimic realistic financial scenarios like periods of constant prices and fat-tailed returns. Sun et al. (2022) studied the parameter estimation for geometric fractional Brownian motion (gfBm) using discrete observations. It emphasizes the effectiveness of gfBm in capturing long-range dependence in stock prices, which is crucial for modeling financial markets, particularly in the context of Chinese financial markets.

Finally, in Section 4, we present a discussion about the weighted sub-fractional Brownian motion process, as well as various related open problems that can be addressed as future work.

## 2. Weighted sub-fractional Brownian motion process

### 2.1. Definition

In this section, we prove a sufficient condition on the function  $f$  for the function (15) to be a covariance function. We, therefore, present a more general definition of weighted sub-fractional Brownian motion. Let

$$R_{f,b}(s, t) := \frac{1}{1-b} \int_0^{s \wedge t} f(r) [(s-r)^b + (t-r)^b - (t+s-2r)^b] dr, \quad s, t \geq 0, \quad (15)$$

where,  $b \in [0, 1) \cup (1, 2]$  and  $f : \mathbb{R}_+ \rightarrow \mathbb{R}_+$  be a measurable function.

**Proposition 1.** *Let  $f : \mathbb{R}_+ \rightarrow \mathbb{R}_+$  be a measurable function such that, for any  $t > 0$*

$$\int_0^t f(u)(t-u)^b du < \infty. \quad (16)$$

*Then,  $R_{f,b}(s, t)$  is a covariance function.*

PROOF. Let  $b \in [0, 1) \cup (1, 2]$  and  $Q_b(s, t) := \frac{1}{1-b} [s^b + t^b - (t+s)^b]$  for  $t, s \geq 0$ .

In Bojdecki et al. (2010) (2.4) it was proved that  $Q_b(s, t)$  is a covariance function. Then, since  $f \geq 0$ ,

$$R_{f,b}(s, t) = \int_0^{s \wedge t} f(r) Q_b(t-r, s-r) dr \quad (17)$$

also is a non-negative definite function. Finally, under the condition (16):

$$\frac{R_{f,b}(t,t)(1-b)}{2-2^b} = \int_0^t f(u)(t-u)^b < \infty, \quad \forall t > 0, \quad (18)$$

and by (18) its easy to check that:

$$|R_{f,b}(s,t)| < \infty.$$

This completes the proof.

**Definition 1.** A centered Gaussian process  $\{\zeta_{t,f,b}, t \geq 0\}$  with covariance function (15) such that  $f$  satisfies the condition (16) is called a weighted sub-fractional Brownian motion.

Consider the family of functions

$$C_1 := \{f_a(u) := u^a \mid u > 0, a > -1\}.$$

For this family, the covariance function can be expressed as follows:

$$C_1(s,t) = \frac{1}{1-b} \int_0^{s \wedge t} u^a [(s-u)^b + (t-u)^b - (t+s-2u)^b] du. \quad (19)$$

Another significant class of functions to consider is:

$$C_2 := \{f_a(u) := e^{au} \mid u > 0, a \in \mathbb{R}\}.$$

For this class, the corresponding covariance function is given by:

$$C_2(s,t) = \frac{1}{1-b} \int_0^{s \wedge t} e^{au} [(s-u)^b + (t-u)^b - (t+s-2u)^b] du. \quad (20)$$

**Remark 1.** For  $-1 < a < 0$ , the covariance function (19) was derived as the covariance function of the rescaled occupation time fluctuations of a  $(d, \alpha, 1, \gamma)$ -branching particle system for the case  $\alpha\gamma < d < \alpha(1 + \gamma)$ , with  $a = \gamma - 1$ . Refer to Theorem 2.1 (i) in López-Mimbela et al. (2024).

## 2.2. Sample paths properties

In this section, we will explore the trajectory properties of the process  $\{\zeta_{t,f,b}, t \geq 0\}$ , including variation, quadratic variation, and the continuity modulus.

**Remark 2.** For  $f \equiv (1-b)^2(1+b)$  we have that

$$R_{f,b}(s, t) = (1-b) \left( t^{b+1} + s^{b+1} - \frac{1}{2} \left[ (t+s)^{b+1} + (t \vee s - t \wedge s)^{b+1} \right] \right) \quad (21)$$

In this case, Bojdecki et al. (2007) proved that  $R_{f,b}(s, t)$  is a covariance function if and only if  $-1 < b \leq 3$ . Additionally, they provided representations for the process  $\zeta_{t,f,b}$ , which are given in Remark 3.

**Remark 3.** (i) Let  $b \in (-1, 1)$  and  $f \equiv c$ , with  $c$  a positive constant. By (2.1) in Bojdecki et al. (2007), the process  $(\zeta_{t,f,b})_{t \geq 0}$  has the following integral representation:

$$\zeta_{t,f,b} = c_{f,b} (\xi_{t,b+1} - \xi_{-t,b+1}), \quad t \geq 0, \quad (22)$$

where  $c_{f,b} := \sqrt{\frac{c}{2(1-b)^2(1+b)}}$  and  $\xi_{t,b+1}$  is fBm defined for all  $-\infty < t < \infty$  with Hurst parameter  $b+1$ .

(ii) Let  $b \in (1, 3]$  and  $f \equiv c$ , with  $c$  a positive constant. By Theorem 3.1 in Bojdecki et al. (2007), the process  $(\zeta_{t,f,b})_{t \geq 0}$  has the following integral representation:

$$\zeta_{t,f,b} = c_{f,b} \int_0^t \nu_{s,b} ds, \quad (23)$$

where  $c_{f,b} := \sqrt{\frac{bc}{2(b-1)}}$  and  $\nu_{t,b}$  is a centered Gaussian process with covariance function  $H_b(s, t) := (s+t)^{b-1} - |s-t|^{b-1}$ .

(iii) If  $b = 0$ , there exists a Gaussian process  $\zeta_{t,f,0}$  with covariance function (19), and the process  $\zeta_{t,f,0} = B \left( \int_0^t f(u) du \right)$ , where  $B(t)$  is a Brownian motion. Therefore, under condition (6), the process  $\zeta_{t,f,0}$  is a square-integrable continuous martingale. Therefore, we assume that  $b \in (0, 1) \cup (1, 2]$ , since for  $\zeta_{t,f,0}$  the analogous results obtained in the rest of the section would be obtained directly from its representation.

Next, we will present theoretical results concerning the variation and quadratic variation of the process  $\zeta_{t,f,b}$  for  $b \in (0, 1) \cup (1, 2]$ . First, we will present

results for the case  $b \in (0, 1)$ . In Bojdecki et al. (2004b) was proved that for  $f \equiv (1 - b)(1 + b)$ . Then,

$$(2 - 2^b)(t - s)^{1+b} \leq E(\zeta_{t,f,b} - \zeta_{s,f,b})^2 \leq (t - s)^{b+1} \quad (24)$$

Let  $T > 0$ , by Lemma 2.1 of Bojdecki et al. (2004a), we have that  $\zeta_{t,f,b}$  has infinite variation and quadratic variation equal to 0 almost surely, over the interval  $[0, T]$ .

From here on, we will use the following notation: given positive real-valued functions  $f$  and  $g$ , we write  $f \asymp g$  if there are positive constants  $c_1$  and  $c_2$  such that  $c_1 f \leq g \leq c_2 f$ . Note that if  $f \asymp g$  with constants  $c_1$  and  $c_2$ , then  $g \asymp f$  with constants  $c_2^{-1}$  and  $c_1^{-1}$ .

**Proposition 2.** *Let  $b \in (0, 1)$ . We suppose that  $1 \asymp f$ . Then, the process  $\zeta_{t,f,b}$  has infinite variation and quadratic variation equal to 0 almost surely, over the interval  $[0, T]$ . In particular, the process  $\zeta_{t,f,b}$  is not a semi-martingale.*

PROOF. It is not difficult to see that:

$$\begin{aligned} \mathbb{E}(\zeta_{t,f,b} - \zeta_{s,f,b})^2 &= \frac{2 - 2^b}{1 - b} \int_s^t f(u)(t - u)^b du \\ &\quad + \frac{1}{1 - b} \int_0^s f(u) [2(t + s - 2u)^b - 2^b(t - u)^b - 2^b(s - u)^b] du \end{aligned} \quad (25)$$

Furthermore, by Jensen's inequality, the function  $u \mapsto \frac{2(t+s-2u)-2^b(t-u)-2^b(s-u)^b}{1-b}$  is non-negative. Due to the assumption  $f \geq 0$ , both terms in (25) are non-negative. Since  $1 \asymp f$ , there exist non-negative constants  $c_{1,f,b}$  and  $c_{2,f,b}$  such that

$$c_{1,f,b}(1 - b)(1 + b) \leq f \leq c_{2,f,b}(1 - b)(1 + b).$$

Thus, from (25) and (24), we have:

$$c_{1,f,b}(2 - 2^b)(t - s)^{1+b} \leq \mathbb{E}(\zeta_{t,f,b} - \zeta_{s,f,b})^2 \leq c_{2,f,b}(t - s)^{b+1} \quad (26)$$

Therefore, by Lemma 2.1 of Bojdecki et al. (2004a), we conclude the proof.  $\square$

**Proposition 3.** *Let  $b \in (0, 1)$ . We suppose that  $u^\alpha \asymp f$  for some  $\alpha \in (-1, \infty)$ . Then, the process  $\zeta_{t,f,b}$  has infinite variation and quadratic variation equal to 0 almost surely, over the interval  $[0, T]$ . In particular, the process  $\zeta_{t,f,b}$  is not a semi-martingale.*

PROOF. Suppose that  $f(u) = u^\alpha$ . It is easy to check that:

$$\begin{aligned}
& \frac{1}{1-b} \int_0^s f(u) \left[ 2(t+s-2u)^b - 2^b(t-u)^b - 2^b(s-u)^b \right] du \\
&= b \int_0^s f(u) \int_s^t \int_s^t \frac{1}{(r+r'-2u)^{2-b}} dr dr' du \\
&= b \int_s^t \int_s^t \int_0^s \frac{u^a}{(r+r')^{2-b}} \frac{1}{(1-\frac{2u}{r+r'})^{2-b}} du dr dr'
\end{aligned} \tag{27}$$

Furthermore, for  $|x| < 1$ , we know that

$$\frac{1}{(1-x)^{2-b}} = \sum_{n=0}^{\infty} \binom{b-2}{n} (-1)^n x^n, \quad \text{where} \quad \binom{b-2}{n} (-1)^n \geq 0 \tag{28}$$

By (27), (28), and following a similar proof to Propositions 2.7 and 2.9 of Ramírez-González et al. (2024b), we have that for  $a \in (-1, 0)$ :

$$\begin{aligned}
& \frac{1}{1-b} \int_0^s f(u) \left[ 2(t+s-2u)^b - 2^b(t-u)^b - 2^b(s-u)^b \right] du \\
&\leq \frac{s^a}{1+a} \cdot \frac{1}{1-b} \int_0^s \left[ 2(t+s-2u)^b - 2^b(t-u)^b - 2^b(s-u)^b \right] du \\
&\leq \frac{s^a}{1+a} \frac{1}{(1-b)(1+b)} (t-s)^{1+b}
\end{aligned} \tag{29}$$

and, on the other hand,

$$\frac{2-2^b}{1-b} \int_s^t f(u)(t-u)^b du \leq \frac{2-2^b}{(1-b)(1+b)} s^a (t-s)^{1+b}$$

Then, by equation (25), we have that

$$\frac{2-2^b}{1-b^2} (t-s)^{1+b} \leq \mathbb{E}(\zeta_{t,f,b} - \zeta_{s,f,b})^2 \leq \frac{1+(2-2^b)(1+a)}{(1+a)(1-b^2)} s^a (t-s)^{1+b} \tag{30}$$

Similarly, for  $a \in (0, \infty)$

$$\frac{2-2^b}{1-b^2} s^a (t-s)^{1+b} \leq \mathbb{E}(\zeta_{t,f,b} - \zeta_{s,f,b})^2 \leq \frac{1}{1-b^2} (t-s)^{1+b}. \tag{31}$$

Furthermore, for the general case  $u^\alpha \asymp f$ , by (25), (30), and (31), we have that there exist positive constants  $c_{1,f}$  and  $c_{2,f}$  such that

$$\frac{2-2^b}{1-b^2} c_{1,f} (t-s)^{1+b} \leq \mathbb{E}(\zeta_{t,f,b} - \zeta_{s,f,b})^2 \leq \frac{1+(2-2^b)(1+a)}{(1+a)(1-b^2)} c_{2,f} s^a (t-s)^{1+b} \quad (32)$$

for  $a \in (-1, 0)$  and in the case  $a \in [0, \infty)$  inequality is satisfied

$$\frac{2-2^b}{1-b^2} c_{1,f} s^a (t-s)^{1+b} \leq \mathbb{E}(\zeta_{t,f,b} - \zeta_{s,f,b})^2 \leq \frac{1}{1-b^2} c_{2,f} (t-s)^{1+b} \quad (33)$$

Finally, by similar arguments to those given in Propositions 2.7 and 2.9 of Ramírez-González et al. (2024b), we conclude the proof.  $\square$

Now, we present results regarding the variation and quadratic variation for the case  $b \in (1, 2]$ . We will demonstrate an integral representation for the process  $\zeta_{t,f,b}$  and thereby establish that it has finite variation.

**Proposition 4.** *(Integral representation for case  $b > 1$ ) Let  $b > 1$  and suppose that exists a positive constant  $c$  and  $a \in (-1, \infty)$  such that  $0 \leq f(u) \leq cu^a$ . Then, the process  $(\zeta_{t,f,b})_{t \geq 0}$  has the following integral representation:*

$$\zeta_{t,f,b} = \sqrt{b} \int_0^t v_{s,f,b} ds \quad (34)$$

where  $(v_{t,f,b})_{t \geq 0}$  is a Gaussian process with covariance function

$$C_{f,b}(s, t) := \int_0^{s \wedge t} f(u) (s+t-2u)^{b-2} du \quad (35)$$

Moreover, when  $a \geq 0$  the process  $(\zeta_{t,f,b})_{t \geq 0}$  is a continuously differentiable process with

$$\frac{d\zeta_{t,f,b}}{dt} = \sqrt{b} v_{t,f,b}$$

PROOF. Its easy to check that:

$$R_{f,b}(s, t) = b \int_0^{s \wedge t} \int_0^{s \vee t} \int_0^{r \wedge v} f(u) (r-u+v-u)^{b-2} du dv dr. \quad (36)$$

Moreover, it is known that

$$t^{b-2} = \frac{1}{\Gamma(2-b)} \int_0^\infty e^{-ut} u^{1-b} du, \text{ for any } t > 0. \quad (37)$$

Then, by (37) it is easy to prove that  $(s, t) \rightarrow (s + t)^{b-2}$  is positive definite function. Consequently, (35) is a covariance function. Therefore, there exists a centered Gaussian process  $(\nu_{t,f,b})_{t \geq 0}$  with covariance function (35). Now, for the integrability of the process  $(\nu_{t,f,b})_{t \geq 0}$ , by Cauchy-Schwarz Inequality it suffices to demonstrate that  $\int_0^t \sqrt{E(\nu_{s,f,b}^2)} ds < \infty$ . Indeed,

$$\begin{aligned} \int_0^t \sqrt{E(\nu_{s,f,b}^2)} ds &\leq 2^{\frac{b-2}{2}} \sqrt{c} \int_0^t \sqrt{\int_0^s u^a (s-u)^{b-2} du} ds \\ &= 2^{\frac{b-2}{2}} \sqrt{cB(a+1, b-1)} \int_0^t s^{\frac{a+b-1}{2}} ds \\ &= 2^{\frac{b}{2}} \frac{\sqrt{cB(a+1, b-1)}}{a+b+1} t^{\frac{a+b+1}{2}} < \infty. \end{aligned}$$

Here,  $B(\cdot, \cdot)$  is the beta function. Therefore, the integral (34) is well defined. Finally, for  $a \geq 0$  we will prove that  $(\nu_{t,f,b})_{t \geq 0}$  has Hölder continuous paths with index  $0 < \delta < \frac{b-1}{2}$ . In particular,  $(\zeta_{t,f,b})_{t \geq 0}$  has continuously differentiable trajectories. Indeed, by Jensen's inequality for  $0 < s \leq t$  and  $0 < u \leq s$  we have that:

$$2^{b-2}(t-u)^{b-2} + 2^{b-2}(s-u)^{b-2} - 2(t+s-2u)^{b-2} \geq 0,$$

and

$$2^{b-1}t^{b-1} + 2^{b-1}s^{b-1} - 2(t+s)^{b-1} \leq 0.$$

Then,

$$\begin{aligned} E(\nu_{t,f,b} - \nu_{s,f,b})^2 &= C_{f,b}(t, t) + C_{f,b}(s, s) - 2C_{f,b}(s, t) \\ &= 2^{b-2} \int_s^t f(u)(t-u)^{b-2} du \\ &\quad + \int_0^s f(u) \left[ 2^{b-2}(t-u)^{b-2} + 2^{b-2}(s-u)^{b-2} - 2(t+s-2u)^{b-2} \right] du \\ &\leq ct^a \left[ \frac{2^{b-2}}{b-1} (t-s)^{b-1} + \frac{2^{b-2}}{b-1} \left( t^{b-1} - (t-s)^{b-1} + s^{b-1} \right) - \frac{1}{b-1} \left( (t+s)^{b-1} - (t-s)^{b-1} \right) \right] \\ &= ct^a \left[ \frac{1}{b-1} (t-s)^{b-1} + \frac{1}{2(b-1)} \left( 2^{b-1}t^{b-1} + 2^{b-1}s^{b-1} - 2(t+s)^{b-1} \right) \right] \leq \frac{ct^a}{b-1} (t-s)^{b-1} \end{aligned} \tag{38}$$

In particular, we have that  $(\nu_{t,f,b})_{t \geq 0}$  has Hölder continuous path of index  $\delta$ , for any  $0 < \delta < \frac{b-1}{2}$ . Therefore, by the Fundamental Theorem of Calculus and (34)

we conclude that  $(\zeta_{t,f,b})_{t \geq 0}$  is a continuously differentiable process with

$$\frac{d\zeta_{t,f,b}}{dt} = \sqrt{b}v_{t,f,b}$$

□

Proposition 4 allows us to define SDEs with respect to the process  $\zeta_{t,f,b}$  for  $b > 1$ , such as those presented in Section 3. On the other hand, results concerning the continuity of the process  $\zeta_{t,f,b}$  are presented in Remark 4.

**Remark 4.** (i) We suppose that there exists a positive constant  $c_f$  such that  $0 \leq f \leq c_f$  on  $[0, T]$  for some  $T > 0$ .

(i.a) For  $b \in [0, 1)$ , by (24) we have that  $(\zeta_{t,f,b})_{t \geq 0}$  has Hölder continuous paths of index  $\delta$ , for any  $0 < \delta < \frac{1+b}{2}$ .

(i.b) For  $b \in (1, 2]$ , by Proposition 3.4 of Bojdecki et al. (2007) exists a positive constant  $c_{1,f,b}$  such that:

$$\mathbb{E}(\zeta_{t,f,b} - \zeta_{s,f,b})^2 \leq c_{1,f,b}(t-s)^2 \quad (39)$$

Then,  $(\zeta_{t,f,b})_{t \geq 0}$  has Hölder continuous paths of index  $\delta$ , for any  $0 < \delta < 1$ .

(ii) Let  $a \in (-1, 0)$ . We suppose that there exists a positive constant  $c_{f,a}$  such that  $0 \leq f \leq c_{f,a}u^a$  on  $[0, T]$  for some  $T > 0$ . By Theorem 2.10 of López-Mimbela et al. (2024), for  $b \in (0, 1) \cup (1, 2]$  there is a positive constant  $c_{f,a,b}(T)$  such that

$$\mathbb{E}(\zeta_{t,f,b} - \zeta_{s,f,b})^2 \leq c_{f,a,b}(T)|t-s|^b, \quad 0 \leq s, t \leq T, \quad (40)$$

In particular, we have that  $(\zeta_{t,f,b})_{t \geq 0}$  has Hölder continuous paths of index  $\delta$ , for any  $0 < \delta < \frac{b}{2}$ . When  $b = 0$ , by Hölder continuity of the function  $x \rightarrow x^{1+a}$ , there is a positive constant  $c_{f,a}(T)$  such that

$$\mathbb{E}(\zeta_{t,f,b} - \zeta_{s,f,b})^2 \leq c_{f,a}(T)|t-s|^{1+a}, \quad 0 \leq s, t \leq T, \quad (41)$$

In particular, we have that  $(\zeta_{t,f,b})_{t \geq 0}$  has Hölder continuous paths of index  $\delta$ , for any  $0 < \delta < \frac{1+a}{2}$ .

**Remark 5.** We suppose that there exists a positive constant  $c_f$  such that  $0 \leq f \leq c_f u^a$  for  $a \in (-1, \infty)$  on  $[0, T]$  for some  $T > 0$ .

(i) For  $b \in (0, 1)$ ,  $(\zeta_{t,f,b})_{t \geq 0}$  is a continuous process of quadratic variation equal to 0.

(ii) For  $b \in (1, 2]$ ,  $(\zeta_{t,f,b})_{t \geq 0}$  is a continuous process of finite variation, it follows that it has quadratic variation equal to 0. Therefore,  $(\zeta_{t,f,b})_{t \geq 0}$  is a semi-martingale.



**Remark 6.** We suppose that there exists a positive constant  $c_f$  such that  $0 \leq f \leq c_f u^a$  for  $a \in (-1, \infty)$  on  $[0, T]$  for some  $T > 0$ .

(i) Let  $b \in (1, 2]$ . Due to the continuity of the process  $\zeta_{t,f,b}$ , its integral representation (34), and by Theorem 31 of Protter (2005), for any function  $f \in C^1([0, T])$ , it holds that  $(f(\zeta_{t,f,b}))_{t \geq 0}$  is of finite variation and

$$f(\zeta_{t,f,b}) - f(\zeta_{0,f,b}) = \int_0^t f'(\zeta_{s,f,b}) d\zeta_{s,f,b}, \quad t \in [0, T]. \quad (42)$$

(ii) Let  $b \in (0, 1)$ . By Proposition 4.1 of Russo and Vallois (2000), we can define a form of integration with respect to  $\{\zeta_{t,f,b}, t \geq 0\}$ . That is: Let  $g \in C^1([0, T])$  and  $G$  such that  $G' = g$ . Then,

$$\int_0^t g(\zeta_{s,f,b}) d^\mp \zeta_{s,f,b} = G(\zeta_{t,f,b}) - G(\zeta_{0,f,b}) \pm \int_0^t g'(\zeta_{s,f,b}) d[\zeta_{\cdot,f,b}, \zeta_{\cdot,f,b}]_s, \quad t \in [0, T]. \quad (43)$$

Here,  $\int_0^t g(\zeta_{s,f,b}) d^- \zeta_{s,f,b}$  is the forward integral,  $\int_0^t g(\zeta_{s,f,b}) d^+ \zeta_{s,f,b}$  is the backward integral and  $\{[\zeta_{\cdot,f,b}, \zeta_{\cdot,f,b}]_t, t \geq 0\}$  is the quadratic variation of  $\{\zeta_{t,f,b}, t \geq 0\}$ .

Additionally, by Proposition 3 we have that  $[\zeta_{\cdot,f,b}, \zeta_{\cdot,f,b}]_t = 0$ . Then,

$$\int_0^t g(\zeta_{s,f,b}) d^\mp \zeta_{s,f,b} = G(\zeta_{t,f,b}) - G(\zeta_{0,f,b}), \quad t \in [0, T]. \quad (44)$$

Next, we proceed to study some memory properties of the process  $\zeta_{t,f,b}$ . In Proposition 5, we study long-range memory properties, and in Propositions 6 and 7 examine short-memory. In Gaussian processes, long memory refers to the persistence of correlations over extended periods, which is vital for modeling phenomena with lasting trends such as in financial markets and hydrology. Conversely, short memory indicates that correlations decay quickly, suitable for processes where only recent values are significant, such as in signal processing and short-term forecasting.

**Proposition 5.** Suppose that  $f$  satisfies condition (6). Then, the process  $\zeta_{f,b}$  satisfies the following properties:

(i) (Long-range memory) For any  $s, t \geq 0$ . If  $b \in [0, 1)$ , then

$$R_{f,b}(s, t + T) \xrightarrow{T \rightarrow \infty} \frac{1}{1-b} \int_0^s f(u)(s-u)^b du \quad (45)$$

and, if  $b \in (1, 2]$

$$\frac{R_{f,b}(s, t + T)}{T^{b-1}} \xrightarrow{T \rightarrow \infty} \frac{b}{b-1} s \int_0^s f(u) du. \quad (46)$$

(ii) (Long-range dependence) Let  $b \in (0, 1) \cup (1, 2]$ . For  $0 < r \leq v$  and  $0 < s \leq t$  it holds that

$$\begin{aligned} \lim_{T \rightarrow \infty} T^{2-b} \mathbb{E} [(\zeta_{v,f,b} - \zeta_{r,f,b})(\zeta_{t+T,f,b} - \zeta_{s+T,f,b})] \\ = b(t-s) \left[ \int_r^v f(u)(v-u)du + (v-r) \int_0^r f(u)du \right]. \end{aligned} \quad (47)$$

Additionally, for  $b = 0$ , it is evidently that  $\mathbb{E} [(\zeta_{v,f,b} - \zeta_{r,f,b})(\zeta_{t+T,f,b} - \zeta_{s+T,f,b})] = 0$ .

PROOF. (i) For  $s, t \geq 0$ . It is easy to check that:

$$R_{f,b}(s, T+t) = \frac{1}{1-b} \int_0^s f(u)(s-u)^b du - \frac{b}{1-b} \int_0^s f(u) \int_t^{t+s} (T+w-2u)^{b-1} dw du \quad (48)$$

Applying the Dominated Convergence Theorem, we obtain (45) and (46). The proof of (ii) follows analogously to the proof of Theorem 2.10 (iv) in López-Mimbela et al. (2024).  $\square$

**Example 1.** Let  $b \in (0, 1) \cup (1, 2]$ . (i) For  $f \in C_1$ , i.e.,  $f(u) = u^a$ ,  $a > -1$ ,

$$\lim_{T \rightarrow \infty} T^{2-b} \mathbb{E} [(\zeta_{tv,f,b} - \zeta_{r,f,b})(\zeta_{t+T,f,b} - \zeta_{s+T,f,b})] = \frac{b(t-s)(v^{a+2} - r^{a+2})}{(a+1)(a+2)}. \quad (49)$$

(ii) For  $f \in C_2$ ,

$$\lim_{T \rightarrow \infty} T^{2-b} \mathbb{E} [(\zeta_{v,f,b} - \zeta_{r,f,b})(\zeta_{t+T,f,b} - \zeta_{s+T,f,b})] = \frac{b(t-s)}{a^2} [(e^{av} - av) - (e^{ar} - ar)]. \quad (50)$$

**Proposition 6.** (i) For  $b = 0$ . Suppose that  $f$  satisfies the condition (6) and is continuous. Then,

$$\lim_{\epsilon \downarrow 0} \frac{\mathbb{E} [(\zeta_{s+\epsilon,f,b} - \zeta_{s,f,b})^2]}{\epsilon} = f(s). \quad (51)$$

(ii) Let  $b \in (0, 1)$  and  $1 \asymp f$  on  $[0, T]$  for some  $T > 0$ . Then, we have

$$\frac{(2-2^b)c_{1,f}}{1-b^2} \leq \liminf_{\epsilon \downarrow 0} \frac{\mathbb{E}(\zeta_{s+\epsilon,f,b} - \zeta_{s,f,b})^2}{\epsilon^{1+b}} \leq \limsup_{\epsilon \downarrow 0} \frac{\mathbb{E}(\zeta_{s+\epsilon,f,b} - \zeta_{s,f,b})^2}{\epsilon^{1+b}} \leq \frac{c_{2,f}}{1-b^2}. \quad (52)$$

Let  $u^a \asymp f$  with  $a \in (0, \infty)$  on  $[0, T]$  for some  $T > 0$ . Then, we have

$$\begin{aligned} \frac{(2-2^b)c_{1,f}}{1-b^2} &\leq \liminf_{\epsilon \downarrow 0} \frac{\mathbb{E}(\zeta_{s+\epsilon,f,b} - \zeta_{s,f,b})^2}{\epsilon^{1+b}} \leq \limsup_{\epsilon \downarrow 0} \frac{\mathbb{E}(\zeta_{s+\epsilon,f,b} - \zeta_{s,f,b})^2}{\epsilon^{1+b}} \\ &\leq \frac{1 + (2-2^b)(1+a)}{(1+a)(1-b^2)} c_{2,f} s^a. \end{aligned} \quad (53)$$

For  $u^a \asymp f$  with  $a \in (-1, 0)$  on  $[0, T]$  for some  $T > 0$ , we have

$$\frac{(2-2^b)c_{1,f}}{1-b^2} s^a \leq \liminf_{\epsilon \downarrow 0} \frac{\mathbb{E}(\zeta_{s+\epsilon,f,b} - \zeta_{s,f,b})^2}{\epsilon^{1+b}} \leq \limsup_{\epsilon \downarrow 0} \frac{\mathbb{E}(\zeta_{s+\epsilon,f,b} - \zeta_{s,f,b})^2}{\epsilon^{1+b}} \leq \frac{c_{2,f}}{1-b^2}. \quad (54)$$

(iii) Let  $b \in (1, 2]$ . Suppose that  $\int_0^\delta f(u)(\delta - u)^{b-2} du < \infty$  for any  $\delta > 0$ . Then, for all  $s > 0$ , we have

$$\lim_{\epsilon \downarrow 0} \frac{\mathbb{E}[(\zeta_{s+\epsilon,f,b} - \zeta_{s,f,b})^2]}{\epsilon^2} = 2^{b-2} b \int_0^s f(u)(s-u)^{b-2} du. \quad (55)$$

PROOF. (i) It is obvious. (ii) It is immediate from the equations (26), (32) and (33). (iii) By L'Hôpital's rule and Dominated Convergence Theorem. We have that:

$$\begin{aligned} \lim_{\epsilon \downarrow 0} \frac{1}{\epsilon^2} \frac{1}{1-b} \int_0^s f(u) \left[ 2(2s+\epsilon-2u)^b - 2^b(s+\epsilon-u)^b - 2^b(s-u)^b \right] du \\ = 2^{b-2} b \int_0^s f(u)(s-u)^{b-2} du. \end{aligned}$$

Also, it is easy to check that  $\lim_{\epsilon \downarrow 0} \frac{1}{\epsilon^2} \frac{2-2^b}{1-b} \int_s^{s+\epsilon} f(u)(s+\epsilon-u)^b du \rightarrow 0$ . Then, by equation (25) we conclude the proof.  $\square$

**Example 2.** Let  $b \in (1, 2]$ . For  $a > -1$ , we consider  $f(u) \equiv u^a$ . Then, for all  $s > 0$

$$\lim_{\epsilon \downarrow 0} \frac{E[(\zeta_{s+\epsilon,f,b} - \zeta_{s,f,b})^2]}{\epsilon^2} = 2^{b-1} b s^{a+b-1} B(a+1, b-1), \quad (56)$$

where  $B(\cdot, \cdot)$  is the function Beta.

**Proposition 7.** Let  $b \in [0, 1) \cup (1, 2]$ . Suppose that  $1 \asymp f$  and  $f$  is continuous at 0. Then,

$$\lim_{\epsilon \downarrow 0} \frac{\mathbb{E}(\zeta_{\epsilon, f, b}^2)}{\epsilon^{1+b}} = \frac{2 - 2^b}{(1 - b)(1 + b)} f(0). \quad (57)$$

Let  $a > -1$ , consider  $f(u) \equiv u^a$ . Then,

$$\lim_{\epsilon \downarrow 0} \frac{\mathbb{E}(\zeta_{\epsilon, f, b}^2)}{\epsilon^{1+b+a}} = \frac{2 - 2^b}{1 - b} B(a + 1, b + 1), \quad (58)$$

PROOF. The proof follows immediately from (25) and the Dominated Convergence Theorem.  $\square$

Finally, we present a continuity theorem for the family of covariance functions  $R_{f,b}(s, t)$  as  $b \rightarrow 1$ .

**Proposition 8.** (Continuity theorem) Let  $s, t \in [0, T]$ , for some  $T > 0$ .

(i) Let  $0 \leq f$  and suppose that  $\int_0^\delta f(u) du < \infty$  for all  $\delta > 0$ . Then,

$$R_{f,b}(s, t) \xrightarrow{b \rightarrow 1} K_f(s, t) \quad (59)$$

where

$$K_f(s, t) := \int_0^{s \wedge t} f(u) \left[ (s + t - 2u) \log(s + t - 2u) - (s - u) \log(s - u) - (t - u) \log(t - u) \right] du. \quad (60)$$

(ii) If  $f \in C_1 \cup C_2$ , then

$$R_{f,b}(s, t) \xrightarrow{(a,b) \rightarrow (0,1)} K_1(s, t). \quad (61)$$

PROOF. (i) For  $s, t \in [0, T]$ , for some  $T > 0$ , it is easy to check that

$$Q_b(t, s) = \frac{1}{1 - b} [s^b + t^b - (t + s)^b] = b \int_0^s \int_0^t \frac{1}{(r + r')^{2-b}} dr dr' \leq \frac{2 - 2^b}{1 - b} T^b. \quad (62)$$

Furthermore, the function  $k : [0, 2] \rightarrow \mathbb{R}_+$  defined by  $k(x) := \frac{2-2^x}{1-x}$  for  $x \in [0, 2]$ ,  $x \neq 1$  and  $k(1) := \lim_{x \rightarrow 1} \frac{2-2^x}{1-x} = 2 \log(2)$  is bounded. Then, there exists a constant  $C_T$  such that  $|Q_b(s, t)| < C_T$  for all  $b \in [0, 1) \cup (1, 2]$ ,  $s, t \in [0, T]$ . Therefore, by (17), L'Hôpital's rule, and the Dominated Convergence Theorem, we conclude the proof of (i). The proof of (ii) is similar to (i).

Under the assumption (6), Ramírez-González et al. (2024b) presented several path and memory properties of the process  $\zeta_f$ , including its variation, quadratic variation, long-range memory, and dependence of the covariance function  $K_f(s, t)$ .

Finally, Figure 9 of supplementary material shows some simulations of the finite-dimensional distributions of the processes  $\zeta_{t,f,b}$  and  $\zeta_{t,f}$  for different functions  $f \in C_1 \cup C_2$ .

### 2.3. Generalization

Let  $d \in \mathbb{N}$  and  $A \subset \mathbb{R}^d$  be a non-empty, measurable, and bounded set. Define  $A_x := \inf\{\|u - x\| \mid u \in A\}$ , where  $\|\cdot\|$  denotes the Euclidean norm on  $\mathbb{R}^d$ , as an extension to the  $d$ -dimensional case. We examine the following covariance structure. Let  $H \in (0, 1]$  and  $f : \mathbb{R}^d \rightarrow \mathbb{R}_+$  be such that for all  $x \in \mathbb{R}^d$ , the following condition is satisfied:

$$\int_{\{u \in \mathbb{R}^d \mid 0 < A_u \leq A_x\}} f(u) \|x - u\|^{2H} du < \infty. \quad (63)$$

Define  $Q_{H,-}(x, y) := \|x\|^{2H} + \|y\|^{2H} - \|x - y\|^{2H}$  and  $Q_{H,+}(x, y) := \|x\|^{2H} + \|y\|^{2H} - \|x + y\|^{2H}$ . It is known that both  $Q_{H,+}(x, y)$  and  $Q_{H,-}(x, y)$  are covariance functions. Therefore, in Proposition 1, an extension for  $R_{f,b}$  in the  $d$ -dimensional case would involve the covariance structure:

$$K_{H,A,f,-}(x, y) := \int_{\{u \in \mathbb{R}^d \mid 0 < A_u \leq A_x \wedge A_y\}} f(u) Q_{H,-}(x - u, y - u) du \quad (64)$$

or

$$K_{H,A,f,+}(x, y) := \int_{\{u \in \mathbb{R}^d \mid 0 < A_u \leq A_x \wedge A_y\}} f(u) Q_{H,+}(x - u, y - u) du. \quad (65)$$

Equation (65) corresponds to  $R_{f,b}$  when considering the space  $\mathbb{R}_+$  instead of  $\mathbb{R}^d$ ,  $A = \{0\}$ , and  $b = 2H$  with  $H \in (0, \frac{1}{2})$ . Alternatively, replacing  $Q_{H,+}$  or  $Q_{H,-}$  with a stationary covariance function  $K(x, y)$ , such as the exponential, Matérn, rational quadratic kernel, etc., modifies the condition (63) to:

$$\int_{\{u \in \mathbb{R}^d \mid 0 < A_u \leq A_x\}} f(u) du < \infty, \quad \forall x \in \mathbb{R}^d. \quad (66)$$

This yields the following covariance structure  $K(x, y)C_{A,f}(x, y)$ , where

$$C_{A,f}(x, y) := \int_{\{u \in \mathbb{R}^d \mid 0 < A_u \leq A_x \wedge A_y\}} f(u) du. \quad (67)$$

In the case of considering the space  $\mathbb{R}_+$  instead of  $\mathbb{R}^d$  and  $A = \{0\}$ ,

$$(x, y) \rightarrow \int_{\{u \in \mathbb{R}_+ | 0 < \|u\| \leq \|x\| \wedge \|y\|\}} f(u) du$$

is the covariance function of  $B\left(\int_0^t f(u) du\right)$ , where  $B(t)$  is a Brownian motion.

**Example 3.** Let  $K(x, y)$  be a stationary covariance function on  $\mathbb{R}^d$ . (i) Consider  $a > -d$  and the function  $f : \mathbb{R}^d \rightarrow \mathbb{R}_+$  given by  $f(u) = \|u\|^a$  and  $A = B(0, 1)$ , the unit ball in  $\mathbb{R}^d$  centered at the origin. Then,

$$C_{A,f}(x, y) = \begin{cases} \frac{2\pi^{\frac{d}{2}}}{\Gamma(\frac{d}{2})(a+d)} [(\|x\| \wedge \|y\|)^{a+d} - 1], & \text{for } \|x\| \wedge \|y\| > 1 \\ 0, & \text{for } \|x\| \wedge \|y\| \leq 1 \end{cases} \quad (68)$$

(ii) Consider  $a \in (-\infty, \infty)$  and the function  $f : \mathbb{R}^d \rightarrow \mathbb{R}_+$ , given by  $f(u) = e^{a\|u\|}$  and  $A = B(0, 1)$ , the unit ball in  $\mathbb{R}^d$  centered at the origin. (ii.a) For  $a < 0$ ,

$$C_{A,f}(x, y) = \begin{cases} \frac{2\pi^{\frac{d}{2}}}{\Gamma(\frac{d}{2})(-a)^d} [\Gamma(d; -a) - \Gamma(d; -a(\|x\| \wedge \|y\|))], & \text{for } \|x\| \wedge \|y\| > 1 \\ 0, & \text{for } \|x\| \wedge \|y\| \leq 1 \end{cases} \quad (69)$$

(ii.b) For  $a > 0$ ,

$$C_{A,f}(x, y) = \begin{cases} \frac{2\pi^{\frac{d}{2}}}{\Gamma(\frac{d}{2})} \int_1^{\|x\| \wedge \|y\|} e^{ar} r^{d-1} dr, & \text{for } \|x\| \wedge \|y\| > 1 \\ 0, & \text{for } \|x\| \wedge \|y\| \leq 1 \end{cases} \quad (70)$$

Consider the covariance functions:  $K_{M,\kappa,\rho}(x, y)$  (Matérn kernel),  $K_{DE,\sigma,\beta}(x, y)$  (double exponential kernel),  $K_{RQ,\sigma,\rho,\kappa}(x, y)$  (rational quadratic kernel), and  $K_{P,\sigma,\rho,\beta}(x, y)$  (periodic kernel). Defined by:

$$K_{M,\kappa,\rho}(x, y) := \frac{\Gamma(\kappa + 1)^{\frac{1}{2}} \kappa^{\frac{\kappa+1}{4}} \|x - y\|^{\frac{\kappa-1}{2}}}{\pi^{\frac{1}{2}} \Gamma(\frac{\kappa+1}{2}) \Gamma(\kappa)^{\frac{1}{2}} (2\kappa^{\frac{1}{2}} \rho)^{\frac{\kappa+1}{2}}} \mathcal{K}_\kappa\left(\frac{\|x - y\|}{\rho}\right) \quad (71)$$

where  $\rho > 0$  and  $\kappa > 0$  are the scale and shape parameters, respectively, and  $\mathcal{K}_\kappa(\cdot)$  is the modified Bessel function of the third kind of order  $\kappa$ .

$$K_{DE,\sigma,\beta}(x, y) := \sigma^2 e^{-\frac{\|x-y\|^2 \beta^2}{2}}, \quad (72)$$

where  $\sigma > 0$  and  $\beta > 0$  are the scale and shape parameters, respectively.

$$K_{RQ,\sigma,\rho,\kappa}(x, y) := \sigma^2 \left( 1 + \frac{\|x - y\|^2}{2\kappa\rho^2} \right)^{-\kappa} \quad (73)$$

where  $\sigma > 0$  and  $\rho > 0$  are the scale and shape parameters, respectively, and  $\kappa > 0$  determines the relative weighting of large-scale and small-scale variations.

$$K_{P,\sigma,\rho,\beta}(x, y) := \sigma^2 e^{-\frac{2 \sin^2\left(\frac{\pi\|x-y\|}{\rho}\right)}{\beta^2}} \quad (74)$$

where  $\sigma > 0$  is a scale parameter,  $\rho > 0$  is a period that determines the distance between repetitions of the function, and  $\beta > 0$  is the length-scale parameter which determines the length-scale function.

Finally, we fix the point  $p = (2, 2) \in \mathbb{R}^2$  and set  $A = B(0, 1) \subset \mathbb{R}^2$  as the unit ball centered at the origin. Figure 10 of supplementary material presents examples of mixed covariance functions associated with equations (64), (65), (67), (71), (72), (73), and (74), evaluated at  $((x, y), p)$ .

### 3. Related Processes

#### 3.1. Weighted sub-fractional Ornstein–Uhlenbeck process

The objective of this section is to present the weighted sub-fractional Ornstein–Uhlenbeck process. We consider two cases for its definition. First, when  $b \in (1, 2]$ , under which  $\zeta_{t,f,b}$  is continuous and of finite variation. Thus, we can use an Itô-type formula to define the weighted sub-fractional Ornstein–Uhlenbeck process. For  $b \in (0, 1)$ , we define the weighted sub-fractional Ornstein–Uhlenbeck process via the forward integral. This process is characterized as the solution to the following stochastic differential equation (SDE):

$$dV_{f,b,t} = -\beta V_{f,b,t} dt + \sigma d\zeta_{t,f,b}, \quad \beta \in (-\infty, \infty), \sigma > 0, \quad t \in [0, T], \text{ for some } T > 0. \quad (75)$$

Let  $b \in (1, 2]$  and  $0 \leq f \leq cu^a$  for some positive constant  $c$  and  $a > -1$  on  $[0, T]$  for some  $T > 0$ . By Remark 6, it is standard to show that (75) has a unique indistinguishable solution, given by:

$$\begin{aligned} V_{f,b,t} &= e^{-\beta t} \left( V_{f,b,0} + \sigma \int_0^t e^{\beta s} d\zeta_{s,f,b} \right) \\ &= e^{-\beta t} \left( V_{f,b,0} + \sigma \sqrt{b} \int_0^t e^{\beta s} \nu_{t,f,b} ds \right), t \in [0, T]. \end{aligned} \quad (76)$$

Assuming that  $V_{f,b,0}$  is known, we have

$$\begin{aligned} H_{f,b}(s, t) &:= \text{cov}(V_{f,b,s}, V_{f,b,t}) \\ &= \sigma^2 b \int_0^s \int_0^t e^{-\beta(s-u)} C_{f,b}(u, v) e^{-\beta(t-v)} dv du, \forall s, t \in [0, T]. \end{aligned} \quad (77)$$

For  $b = 0$ , by Remark 3 (iii) and Itô formula the unique solution of (75) given by the first equality of (76).

For the case  $b \in (0, 1)$  or covariance function (60) (see Remark 2.10 of Ramírez-González et al. (2024b)), we consider the forward integral of the SDE:

$$d^- V_{f,b,t} = -\beta V_{f,b,t} dt + \sigma d^- \zeta_{t,f,b}, \quad \mu \in (-\infty, \infty), \sigma > 0, \quad t \in [0, T], \quad (78)$$

From Section 4 and Section 5 of Russo and Vallois (2000) it is easy to check that the unique solution of (78) is given by:

$$\begin{aligned} V_{f,b,t} &= e^{-\beta t} \left( V_{f,b,0} + \sigma \int_0^t e^{\beta s} d^- \zeta_{s,f,b} \right) \\ &= e^{-\beta t} V_{f,b,0} + \sigma \zeta_{t,f,b} - \sigma \beta \int_0^t e^{-\beta(t-s)} \zeta_{s,f,b} ds. \end{aligned} \quad (79)$$

Furthermore, assuming that  $V_{f,b,0}$  is known, we have:

$$\begin{aligned} H_{f,b}(s, t) &:= \sigma^2 R_{f,b}(s, t) - \sigma^2 \beta \left( \int_0^s e^{-\beta(s-u)} R_{f,b}(u, t) du + \int_0^t e^{-\beta(t-v)} R_{f,b}(v, s) dv \right) \\ &\quad + \sigma^2 \beta^2 \int_0^s \int_0^t e^{-\beta(s-u)} R_{f,b}(u, v) e^{-\beta(t-v)} dv du. \end{aligned} \quad (80)$$

Therefore,  $(V_{f,b,t})_{t \geq 0}$  is a Gaussian process with mean function  $m_{f,b}(t) := e^{-\beta t} V_{f,b,0}$  and covariance function  $H_{f,b}$ .

**Remark 7.** Let  $0 \leq f \leq cu^a$  for some positive constant  $c$  and  $a > -1$  on  $[0, T]$ . Considering the covariance function (60), by Proposition 2.7 of Ramírez-González et al. (2024b), we have that  $\zeta_{t,f}$  has quadratic variation equal to 0. Therefore, we can define the Ornstein-Uhlenbeck process with respect to  $\zeta_{t,f}$  analogously to the definition given in the case  $b \in (0, 1)$ .

In Section 3.3 Part (i), we present a method for simulating the process  $(V_{f,b,t})_{t \geq 0}$  using its finite-dimensional distributions.



### 3.2. Geometric weighted sub-fractional Brownian motion

Our objective in this section is to define the geometric weighted sub-fractional Brownian motion process for the case  $b \in [0, 1) \cup (1, 2]$ . For  $b \in (1, 2]$ , we will utilize the integral representation (34) and the equation (42). Let  $0 \leq f \leq cu^a$  for some positive constant  $c$  and  $a > -1$  on  $[0, T]$ . We define the geometric weighted sub-fractional Brownian motion process  $S_{t,f,b}$  as the solution to the following stochastic differential equation (SDE):

$$dS_{t,f,b} = \mu S_{t,f,b} dt + \sigma S_{t,f,b} d\zeta_{t,f,b}, \quad \mu \in (-\infty, \infty), \sigma > 0, \quad t \in [0, T], \quad (81)$$

where  $\mu$  is the "percentage drift" and  $\sigma$  is the "percentage volatility". By (42), it is standard to show that (81) has a unique indistinguishable solution, given by:

$$S_{t,f,b} = S_{0,f,b} e^{\mu t + \sigma \zeta_{t,f,b}}, \quad t \in [0, T]. \quad (82)$$

For the case  $b \in (0, 1)$  or covariance function (60) (see Remark 2.10 of Ramírez-González et al. (2024b)), we consider the forward integral of the SDE:

$$d^- S_{t,f,b} = \mu S_{t,f,b} dt + \sigma S_{t,f,b} d^- \zeta_{t,f,b}, \quad \mu \in (-\infty, \infty), \sigma > 0, \quad t \in [0, T], \quad (83)$$

in Section 5 of Russo and Vallois (2000) its proved that the unique solution of (83) is given by (82).

For  $b = 0$ , by Ito's integration we obtain that:

$$S_{t,f,b} = S_{0,f,b} e^{\mu t - \frac{\sigma^2}{2} \int_0^t f(s) ds + \sigma \zeta_{t,f,b}}, \quad t \in [0, T]. \quad (84)$$

In Section 3.3 Part (ii), we present a method for simulating the process  $(S_{t,f,b})_{t \geq 0}$  using its finite-dimensional distributions.

### 3.3. Simulation paths

**Part (i): Simulation of weighted sub-fractional Ornstein-Uhlenbeck process.**

Our objective in this section is to provide a method for calculating the covariance function  $H_{f,b}(s, t)$ . Let  $0 \leq f \leq cu^a$  for some positive constant  $c$  and  $a > -1$  on  $[0, T]$  for some  $T > 0$ ,  $n \in \mathbb{N}$ , and  $\bar{t} = (t_0 := 0, \dots, t_n := T)$ , a partition of the interval  $[0, T]$  into  $n$  blocks. We define  $\Delta_k := t_k - t_{k-1}$  for  $k = 1, \dots, n$ . To numerically calculate double integrals, it is more efficient if both integrals are over regions of similar length, and these regions are as small as possible. The efficiency and accuracy of numerical integration methods, such as quadrature rules, are influenced by the size of the integration region. Smaller integration regions reduce

computational complexity and error. Therefore, we consider the following matrix decompositions.

For  $b \in (1, 2]$ , it is easy to see that:

$$\begin{aligned} & \int_0^{t_i} \int_0^{t_j} e^{-\beta(t_i-u)} R_{f,b}(u, v) e^{-\beta(t_j-v)} dv du \\ &= \sum_{k_1=1}^i \sum_{k_2=1}^j e^{-\beta(t_i-t_{k_1})} G_{f,b}^{(1)}(k_1, k_2) e^{-\beta(t_j-t_{k_2})}, \quad i, j = 1, \dots, n \end{aligned} \quad (85)$$

where  $G_{f,b}^{(1)}(i, j)$  is a matrix of dimensions  $n \times n$  defined by:

$$G_{f,b}^{(1)}(i, j) := \int_0^{\Delta_i} \int_0^{\Delta_j} e^{-\beta u} C_{f,b}(t_i - u, v + t_j - v) e^{-\beta v} dv du, \quad i, j = 1, \dots, n$$

We define  $B$  a lower triangular matrix as  $B(i, j) := e^{-\beta(t_i-t_j)}$ ,  $i, j = 1, \dots, n$ . Then,

$$H_{f,b}(t_i, t_j) = \sigma^2 b (B \cdot G_{f,b}^{(1)} \cdot B^t)(i, j) \quad (86)$$

Then, it is more numerically efficient to compute the finite-dimensional distributions of  $V_{f,b,t}$  using equation (86) rather than directly from equation (77).

Now, for  $b \in [0, 1)$ . Its easy to check that:

$$\int_0^{t_i} e^{-\beta(t_i-u)} R_{f,b}(u, t_j) du = \sum_{k=1}^i e^{-\beta(t_i-t_k)} D_{f,b}(k, j), \quad i, j = 1, \dots, n$$

where  $D_{f,b}(i, j)$  is a matrix of dimensions  $n \times n$  defined by:

$$D_{f,b}(i, j) := \int_0^{\Delta_i} e^{-\beta u} R_{f,b}(t_i - u, t_j) du, \quad i, j = 1, \dots, n$$

and

$$\begin{aligned} & \int_0^{t_i} \int_0^{t_j} e^{-\beta(t_i-u)} R_{f,b}(u, v) e^{-\beta(t_j-v)} dv du \\ &= \sum_{k_1=1}^i \sum_{k_2=1}^j e^{-\beta(t_i-t_{k_1})} G_{f,b}^{(2)}(k_1, k_2) e^{-\beta(t_j-t_{k_2})}, \quad i, j = 1, \dots, n \end{aligned}$$

where  $G_{f,b}^{(2)}(i, j)$  is a matrix of dimensions  $n \times n$  defined by:

$$G_{f,b}^{(2)}(i, j) := \int_0^{\Delta_i} \int_0^{\Delta_j} e^{-\beta u} R_{f,b}(t_i - u, v + t_j - v) e^{-\beta v} dv du, \quad i, j = 1, \dots, n$$

Then,

$$\begin{aligned} H_{f,b}(t_i, t_j) = \sigma^2 & \left[ R_{f,b}(t_i, t_j) - \beta \left( \sum_{k=1}^i e^{-\beta(t_i - t_k)} D_{f,b}(k, j) + \sum_{k=1}^j e^{-\beta(t_j - t_k)} D_{f,b}(k, i) \right) \right. \\ & \left. + \beta^2 \sum_{k_1=1}^i \sum_{k_2=1}^j e^{-\beta(t_i - t_{k_1})} G_{f,b}^{(2)}(k_1, k_2) e^{-\beta(t_j - t_{k_2})} \right] \end{aligned}$$

Therefore,

$$H_{f,b}(t_i, t_j) = \sigma^2 \left[ R_{f,b} - \beta \left( B \cdot D_{f,b} + (B \cdot D_{f,b})^t \right) + \beta^2 B \cdot G_{f,b}^{(2)} \cdot B^t \right] (i, j) \quad (87)$$

Again, it is more numerically efficient to compute the finite-dimensional distributions of  $V_{f,b,t}$  using equation (87) rather than directly from equation (80).

**Part (ii): Simulation of geometric weighted sub-fractional Brownian motion.**

Let  $0 \leq f \leq cu^a$  for some positive constant  $c$  and  $a > -1$  on  $[0, T]$ , for some  $T > 0$ . Consider the process

$$X_{t,f,b} := \log \left( \frac{S_{t,f,b}}{S_{0,f,b}} \right) = \begin{cases} \mu t + \sigma \zeta_{t,f,b}, & \text{for } b \in (0, 1) \cup (1, 2] \\ \mu t - \frac{\sigma^2}{2} \int_0^t f(s) ds + \sigma \zeta_{t,f,b}, & \text{for } b = 0 \end{cases} \quad (88)$$

We have that the process  $(X_{t,f,b})_{t \geq 0}$  is a Gaussian process. Therefore, we can use its finite-dimensional distributions to perform inference and simulations on the process  $S_{t,f,b}$ . Finally, in Figures 11 and 12 of supplementary material, we present simulations of the processes  $(V_{f,b,t})_{t \geq 0}$  and  $(S_{t,f,b})_{t \geq 0}$ , respectively.

#### 4. Discussion and future work

We have presented several path properties, simulations, inferences, and generalizations of the weighted sub-fractional Brownian motion. Notably, we highlight the flexibility of measurable functions  $f : \mathbb{R}_+ \rightarrow \mathbb{R}_+$  that satisfy condition (8).

As future work, we plan to determine the necessary and sufficient conditions for the function (3) to be a covariance function in the remaining cases. Additionally, we propose applying the family of covariance functions  $R_{f,b}(s, t)$  to model real-world data. For example, Ramírez-González et al. (2024b) presented an application where they modeled the animal telemetry of bats with immigration tendencies using the centered Gaussian process  $\zeta_{t,f}$  with covariance function  $K_f(s, t)$ , where  $f \in C_2$ . By Theorem 8,  $R_{f,b}(s, t)$  is a robust family of covariance functions for  $K_f(s, t)$ , which can be used to model animal telemetry with immigration.

In Section 2.3, we extend these generalizations to the space  $\mathbb{R}^d$ . For future work, we propose to develop path properties of the Gaussian process with covariance function (64), (65), or (67), as well as making applications to model real-world data.

Another interesting point would be to introduce correlation structures in the weighted sub-fractional Brownian motion, as presented by Lavancier et al. (2009) and Amblard et al. (2013) for the fractional Brownian motion. By introducing correlation structures in the weighted sub-fractional Brownian motion, we could extend these structures to the weighted sub-fractional Ornstein–Uhlenbeck process and define it in a multidimensional context. This approach would allow for applications similar to those presented by Ramírez-González et al. (2024a), where they studied the correlation in three-dimensional animal telemetry data assuming that the velocity of the animal telemetry follows a 3D-dimensional fractional Ornstein–Uhlenbeck process.

Additionally, we propose studying the theoretical properties of trajectories of the weighted sub-fractional Ornstein–Uhlenbeck process, as well as its possible applications mentioned in Section 1. For parameter inference, using Least Squares Estimation (LSE) on the SDE (75) with  $\beta > 0$ , and based on (18) and Remark 4, it is clear that hypotheses  $(\mathcal{H}_1)$  and  $(\mathcal{H}_2)$  of Theorem 6.1 in Alsenafi et al. (2021) are satisfied. Therefore,

$$\hat{\beta}_{t,f,b} := \frac{V_{f,b,t}^2}{2 \int_0^t V_{f,b,t}^2 ds} \quad (89)$$

is a consistent estimator for  $\beta$ . However, computationally, we cannot calculate it as it requires the entire trajectory of the process  $(V_{f,b,t})_{t \in [0, \infty)}$ . Therefore, we need to study a discrete version of the estimator  $\hat{\beta}_{t,f,b}$ , such as:

$$\hat{\beta}_n := \frac{\sum_{i=1}^n V_{f,b,t_{i-1}} (V_{f,b,t_i} - V_{f,b,t_{i-1}})}{\Delta_n \sum_{i=1}^n V_{f,b,t_{i-1}}^2}, \quad \tilde{\beta}_n := \frac{V_{f,b,T_n}^2}{2\Delta_n \sum_{i=1}^n V_{f,b,t_{i-1}}^2} \quad (90)$$

In Alsenafi et al. (2021), it is shown that the estimators given in (90) are consistent for the Ornstein–Uhlenbeck process associated with the weighted fractional Brownian motion (see equation (1)).

Finally, as future work, we propose to explore applications mentioned in the introduction, specifically those related to the weighted sub-fractional Ornstein–Uhlenbeck processes and geometric weighted sub-fractional Brownian motion.

## 5. Supplementary Material

### 5.1. Numerical Studies

The objective of this section is to compare various numerical integration methods for calculating the integral (7). Our goal is to optimize the execution time required to compute the finite-dimensional distributions of the process  $\zeta_{t,f,b}$  over the family of functions  $C_1 \cup C_2$ . Additionally, we consider the pressure of the calculations performed in the methods.

We implemented simulations of the finite-dimensional distributions of the process  $\zeta_{t,f,b}$  using the R programming language. Four different numerical integration methods were evaluated. The first method, *Integration Method with Gauss-Kronrod and Wynn's Epsilon Algorithm*, employs a globally adaptive interval subdivision technique coupled with extrapolation using Wynn's Epsilon algorithm to improve accuracy. The core of this method is the Gauss-Kronrod quadrature, which enhances the precision of numerical integration by extending the nodes of the Gauss quadrature (see Piessens et al. (1983)), and it is implemented in the R Project within the "stats" package using the "integrate" function. The second method, *h-adaptive multivariate integration over hypercubes*, utilizes an adaptive integration technique based on the multidimensional extension of Clenshaw-Curtis quadrature rules. This approach repeatedly subdivides the integration domain and applies the Clenshaw-Curtis quadrature, adjusting the partitioning to ensure the error remains within the specified tolerance, and is implemented in the R Project within the "cubature" package using the "hcubature" function (see Genz and Malik (2023)). The third method, *p-adaptive multivariate integration over hypercubes*, repeatedly increases the degree of quadrature rules until convergence is achieved, utilizing a tensor product of Clenshaw-Curtis quadrature rules. Further details can be found in the "cubature" package documentation in the R Project, and this method is implemented through the "pcubature" function (see Genz and Malik (2023)). Finally, the fourth method focuses on developing the integral (7) using known functions, aiming to express the integral in terms of well-established

functions, as presented in Table 1. In doing so, we use the optimal numerical algorithms that have been developed for these functions.

Function	Representation	R function	R package
Beta function	$B(a, b)$	beta(a,b)	base package
Incomplete Beta function	$IB(x; a, b)$	lbeta(x,a,b)	spsb
Gamma function	$\Gamma(b)$	gamma(b)	base package
Upper incomplete Gamma function	$\Gamma(x; b)$	gammainc(b,x)	pracma
Hypergeometric function of the first kind	${}_1F_1(x; a, b)$	exp(chf_1F1(x,a,b))	scModels
Hypergeometric function	${}_2F_1(x; a, b, c)$	hypergeo(a,b,c,x)	hypergeo
Exponential integration function	$Ei(x)$	expint_Ei(x)	expint

Table 1: Functions in the R Project software used to numerically calculate the finite-dimensional distributions of the process  $\zeta_{f,b}$  according to Method 4.

For  $b \in [0, 1) \cup (1, 2]$ , we initiate the development of the integral (15) in terms of the functions listed in Table 1, for functions  $f \in C_1 \cup C_2$ . Indeed,

**Case  $f \in C_1$ :**

$$\begin{aligned}
R_{f,b}(s, t) &= \frac{1}{1-b} \int_0^{s \wedge t} r^a [(s-r)^b + (t-r)^b - (t+s-2r)^b] dr \\
&= \frac{1}{1-b} \left[ (s \wedge t)^{a+b+1} B(a+1, b+1) + (s \vee t)^{a+b+1} IB\left(\frac{s \wedge t}{s \vee t}; a+1, b+1\right) \right. \\
&\quad \left. - 2^{-a-1} (s \wedge t + s \vee t)^{a+b+1} IB\left(\frac{2s \wedge t}{s \wedge t + s \vee t}; a+1, b+1\right) \right]
\end{aligned} \tag{1a}$$

where

$$IB(x; a, b) := \int_0^x u^{a-1} (1-u)^{b-1} du, \text{ for } x \in [0, 1], \text{ and } a, b \geq 0,$$

is the Incomplete Beta Function.

**Case  $f \in C_2$ :** Let  $a > 0$ , its easy to check that

$$\int_0^x e^{au}(1-u)^b du = e^a a^{-b-1} \left( \Gamma(a(1-x); b+1) - \Gamma(a; b+1) \right), \quad x \in [0, 1], \quad (91)$$

where

$$\Gamma(x; b) := \int_x^\infty u^{b-1} e^{-u} du, \quad \text{for } x \in (0, \infty), \text{ and } b \geq 0,$$

is the upper Incomplete Gamma Function. Then,

$$\begin{aligned} R_{f,b}(s, t) &= \frac{1}{1-b} \int_0^{s \wedge t} e^{ar} \left[ (s-r)^b + (t-r)^b - (t+s-2r)^b \right] dr \\ &= \frac{1}{(1-b)a^{b+1}} \left[ e^{a(s \wedge t)} \left( \Gamma(b+1) - \Gamma(a(s \wedge t); b+1) \right) + e^{a(s \vee t)} \left( \Gamma(a(s \vee t - s \wedge t); b+1) \right. \right. \\ &\quad \left. \left. - \Gamma(a(s \vee t); b+1) \right) - 2^b e^{a \frac{s \vee t + s \wedge t}{2}} \left( \Gamma\left(a \frac{s \vee t - s \wedge t}{2}; b+1\right) - \Gamma\left(a \frac{s \vee t + s \wedge t}{2}; b+1\right) \right) \right] \end{aligned} \quad (2a)$$

Let  $a < 0$ , its easy to check that

$$\int_0^x e^{au}(1-u)^b du = \frac{e^a}{a} (-a)^{-b} \left( \int_0^{a(x-1)} u^b e^u du - \int_0^{-a} u^b e^u du \right), \quad x \in [0, 1],$$

and

$$\int_0^x u^b e^u du = \frac{x^{b+1}}{b+1} {}_1F_1(x; b+1, b+2), \quad x \geq 0.$$

where

$${}_1F_1(x; a, b) := \frac{\Gamma(a)}{\Gamma(b-a)\Gamma(a)} \int_0^1 e^{xu} u^{a-1} (1-u)^{b-a-1} du, \quad \text{for } x \in (-\infty, \infty), \text{ and } a > 0, b > a,$$

is the confluent hypergeometric function of the first kind. Then,

$$\int_0^x e^{au}(1-u)^b du = \frac{e^a}{b+1} \left( {}_1F_1(-a; b+1, b+2) - (1-x)^{b+1} {}_1F_1(a(x-1); b+1, b+2) \right) \quad (3a)$$

Therefore,

$$\begin{aligned}
R_{f,b}(s, t) &= \frac{1}{1-b} \int_0^{s \wedge t} e^{ar} [(s-r)^b + (t-r)^b - (t+s-2r)^b] dr \\
&= \frac{1}{1-b^2} \left[ e^{a(s \wedge t)} (s \wedge t)^{b+1} {}_1F_1(-a(s \wedge t); b+1, b+2) \right. \\
&\quad + e^{a(s \vee t)} \left( (s \vee t)^{b+1} {}_1F_1(-a(s \vee t); b+1, b+2) \right. \\
&\quad \left. - (s \vee t - s \wedge t)^{b+1} {}_1F_1(-a(s \vee t - s \wedge t); b+1, b+2) \right) \\
&\quad \left. - 2^b e^{a \frac{s \vee t + s \wedge t}{2}} \left( \left( \frac{s \wedge t + s \vee t}{2} \right)^{b+1} {}_1F_1\left(-a \frac{s \vee t + s \wedge t}{2}; b+1, b+2\right) \right. \right. \\
&\quad \left. \left. - \left( \frac{s \vee t - s \wedge t}{2} \right)^{b+1} {}_1F_1\left(-a \frac{s \vee t - s \wedge t}{2}; b+1, b+2\right) \right) \right]
\end{aligned} \tag{4a}$$

Next, we will compare the execution time of each of the four methods described earlier, which are used to calculate the finite-dimensional distributions associated with the centered Gaussian process  $\zeta_{t,f,b}$ . Let  $T > 0$ ,  $n \in \mathbb{N}$ , and  $\bar{t} = (t_0 := 0, \dots, t_n := T)$ , be a partition of the interval  $[0, T]$  into  $n$  blocks. We define  $\Delta_k := t_k - t_{k-1}$  for  $k = 1, \dots, n$ . For the following simulations, we consider  $T = 10$ ,  $n = 100, 200, \dots, 1500$ ,  $\Delta_k = \Delta := \frac{T}{n}$ , for  $k = 1, \dots, n$ .

In Figure 1, panel (a), we observe that for  $f \in C_1$ , Method 4 proves to be the most efficient, followed by Method 1. The execution time ratios between Method 1 and Method 4, shown in panel (d) (blue line), indicate an average execution time ratio of 4.41709. This means that, in the simulations conducted, Method 4 is in average execution time 441.7097% faster than Method 1. This demonstrates the superior efficiency of Method 4 in our simulations. Additionally, the maximum coordinate-wise differences in the covariance matrix calculations of the finite-dimensional distributions, comparing the four methods, were of the order of  $10^{-4}$ . Therefore, it is recommended to calculate the finite-dimensional distributions using Method 4. That is, through the equation (1a) and Table 1.

Now, for  $f \in C_2$ , we consider two sub-cases. When  $a > 0$  (panel (b)), the results are similar to those reported for  $f \in C_1$ . In the simulations conducted, Method 4 is in average execution time 224.0379% faster than Method 1 (panel (d),



red line). However, when  $a < 0$ , Method 1 proves to be the most efficient, followed by Method 3 (panel (c)). In the simulations conducted, Method 1 is in average execution time 206.0608% faster than Method 3. Again, in both sub-cases, the maximum coordinate-wise differences in the covariance matrix calculations of the finite-dimensional distributions, comparing the four methods, were of the order of  $10^{-4}$ . Therefore, we recommend using equation (2a) and Table 1 when  $a > 0$ , and using Method 1 when  $a < 0$  for calculating the finite-dimensional distributions of  $\zeta_{t,f,b}$ .

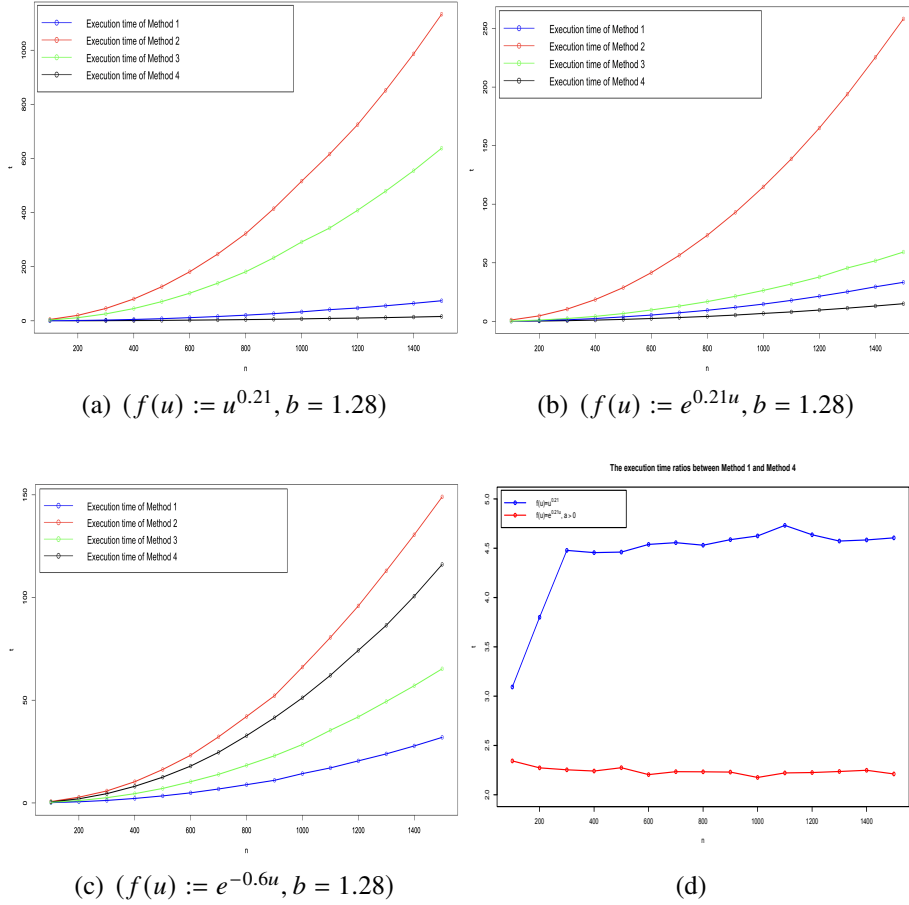


Figure 1: Panel (a), (b), and (c) represent the execution time of calculating the covariance function associated with the process  $\zeta_{t,f,b}$  over the time vector  $\bar{t}$ . Panel (d) shows the execution time ratios between Method 1 and Method 4 for Panels (a) and (b).

Additionally, we conducted a similar simulation study for calculating the covariance matrix of the finite-dimensional distributions of the process  $\zeta_{t,f}$  over the family of functions  $C_1 \cup C_2$ . For this, we need to compute the covariance function  $K_f(s, t)$  in terms of the functions in Table 1, for  $f \in C_1 \cup C_2$ . Indeed,

**Case  $f \in C_1$  and covariance function  $K_f(s, t)$ :** For  $x \in [0, 1]$ , we have that:

$$\int_0^x u^a (1-u) \log(1-u) du = -\frac{1}{(a+1)(a+2)(a+3)} x^{a+1} \left[ (a+1)x^2 {}_2F_1(x; 1, a+3, a+4) \right. \\ \left. - (a+3)x {}_2F_1(x; 1, a+2, a+3) + (a+3) \left( a(x-1) + x - 2 \right) \log(1-x) \right] \quad (5a)$$

where

$${}_2F_1(x; a, b, c) := \frac{\Gamma(c)}{\Gamma(b)\Gamma(c-b)} \int_0^1 \frac{u^{b-1} (1-u)^{c-b-1}}{(1-ux)^a} du, \quad x \in [0, 1], 0 < b \leq c \text{ and } a \in (-1, \infty)$$

is the hypergeometric function. We define  $r_a := \int_0^1 u^a (1-u) \log(1-u) du$ , for  $a \in (-1, \infty)$  and additionally its easy to check that:

$$K_f(s, t) = \int_0^{s \wedge t} u^a [(s+t-2u) \log(s+t-2u) - (s-u) \log(s-u) - (t-u) \log(t-u)] du \\ = 2^{-a-1} (s \vee t + s \wedge t)^{a+2} \left[ \log(s \vee t + s \wedge t) IB\left(\frac{2s \wedge t}{s \vee t + s \wedge t}; a+1, 2\right) \right. \\ \left. + \int_0^{\frac{2s \wedge t}{s \vee t + s \wedge t}} u^a (1-u) \log(1-u) du \right] \\ - (s \vee t)^{a+2} \left[ \log(s \vee t) IB\left(\frac{s \wedge t}{s \vee t}, a+1, 2\right) + \int_0^{\frac{s \wedge t}{s \vee t}} u^a (1-u) \log(1-u) du \right] \\ - (s \wedge t)^{a+2} \left[ \log(s \wedge t) B(a+1, 2) + r_a \right] \quad (6a)$$

By equations (5a) and (6a) the covariance function  $K_f(s, t)$  can be expressed in terms of the functions  $\log(\cdot)$ ,  $IB(\cdot; a, b)$  and  ${}_2F_1(\cdot; a, b, c)$ .

**Case  $f \in C_2$  and covariance function  $K_f(s, t)$ :** For  $x \in [0, 1]$ , if  $a > 0$

$$\int_0^x e^{au}(1-u) \log(1-u) du = \frac{e^{ax} \left( (a(1-x) + 1) \log(1-x) + 1 \right) + e^a \Gamma(a(1-x); 0) - (1 + e^a \Gamma(a; 0))}{a^2}. \quad (7a)$$

If  $a < 0$

$$\int_0^x e^{au}(1-u) \log(1-u) du = \frac{e^{ax} \left( (a(1-x) + 1) \log(1-x) + 1 \right) + e^a G_a(x) - 1}{a^2} \quad (8a)$$

Here,

$$G_a(x) := \int_{a(x-1)}^{-a} \frac{e^u}{u} du = Ei(-a) - Ei(a(x-1)),$$

where  $Ei(\cdot)$  is the exponential integral function. We define  $\gamma_{1,a} := \int_0^1 e^{au}(1-u) du$  and  $\gamma_{2,a} := \int_0^1 e^{au}(1-u) \log(1-u) du$ . Then,

$$\begin{aligned} K_f(s, t) &= \int_0^{s \wedge t} e^{au} [(s+t-2u) \log(s+t-2u) - (s-u) \log(s-u) - (t-u) \log(t-u)] du \\ &= 2^{-1} (s \vee t + s \wedge t)^2 \left[ \log(s \vee t + s \wedge t) \int_0^{\frac{2s \wedge t}{s \vee t + s \wedge t}} e^{a \frac{s \wedge t + s \vee t}{2} u} (1-u) du \right. \\ &\quad \left. + \int_0^{\frac{2s \wedge t}{s \vee t + s \wedge t}} e^{a \frac{s \wedge t + s \vee t}{2} u} (1-u) \log(1-u) du \right] - (s \vee t)^2 \left[ \log(s \vee t) \int_0^{\frac{s \wedge t}{s \vee t}} e^{a(s \vee t)u} (1-u) du \right. \\ &\quad \left. + \int_0^{\frac{s \wedge t}{s \vee t}} e^{a(s \vee t)u} (1-u) \log(1-u) du \right] - (s \wedge t)^2 \left[ \log(s \wedge t) \gamma_{1,a(s \wedge t)} + \gamma_{2,a(s \wedge t)} \right] \end{aligned} \quad (9a)$$

Its easy to check that: For  $a \in (-\infty, \infty)$ ,  $a \neq 0$

$$\gamma_{1,a} = \int_0^1 e^{au}(1-u) du = \frac{e^a - (1+a)}{a^2},$$

for  $a > 0$

$$\gamma_{2,a} = \int_0^1 e^{au}(1-u) \log(1-u) du = -\frac{e^a \left( \Gamma(a; 0) + \gamma - 1 + \log(a) + e^{-a} \right)}{a^2}$$

and for  $a < 0$

$$\gamma_{2,a} = \int_0^1 e^{au} (1-u) \log(1-u) du = -\frac{e^a \left( -Ei(-a) + \gamma - 1 + \log(-a) + e^{-a} \right)}{a^2}$$

By equations (7a) and (8a) the covariance function  $K_f(s, t)$  can be expressed in terms of the functions  $\log(\cdot)$ ,  $\Gamma(\cdot; a)$ ,  ${}_1F_1(\cdot; a, b, c)$  and  $Ei(\cdot)$ .

We will compare the execution time of each of the four methods described earlier, which are used to calculate the finite-dimensional distributions associated with the centered Gaussian process  $\zeta_{t,f}$ .

In Figure 2, panel (a), we observe that for  $f \in C_1$ , Method 1 proves to be the most efficient, followed by Method 3 (panel (a)). In the simulations conducted, The execution time ratios between Method 3 and Method 1, indicate that Method 1 is in average execution time 1090.947% faster than Method 1, and the maximum coordinate-wise differences in the covariance matrix calculations of the finite-dimensional distributions, comparing the four methods, were of the order of  $10^{-4}$ . Therefore, we recommend using Method 1 for calculating the finite-dimensional distributions of  $\zeta_{t,f}$ .

Now, for  $f \in C_2$ , we consider two sub-cases:  $a > 0$  (panel (b)) and  $a < 0$  (panel (c)). In both cases, Method 4 proves to be the most efficient, followed by Method 1. The execution time ratios between Method 1 and Method 4 (panel (d), blue and red lines, respectively) indicate that Method 4 is, on average, 150.6627% and 161.3629% faster than Method 1, respectively. Again, in both sub-cases, the maximum coordinate-wise differences in the covariance matrix calculations of the finite-dimensional distributions, comparing the four methods, were of the order of  $10^{-4}$ . Therefore, we recommend using equations (7a), (8a), (9a), and Table 1 for calculating the finite-dimensional distributions of  $\zeta_{t,f}$ .

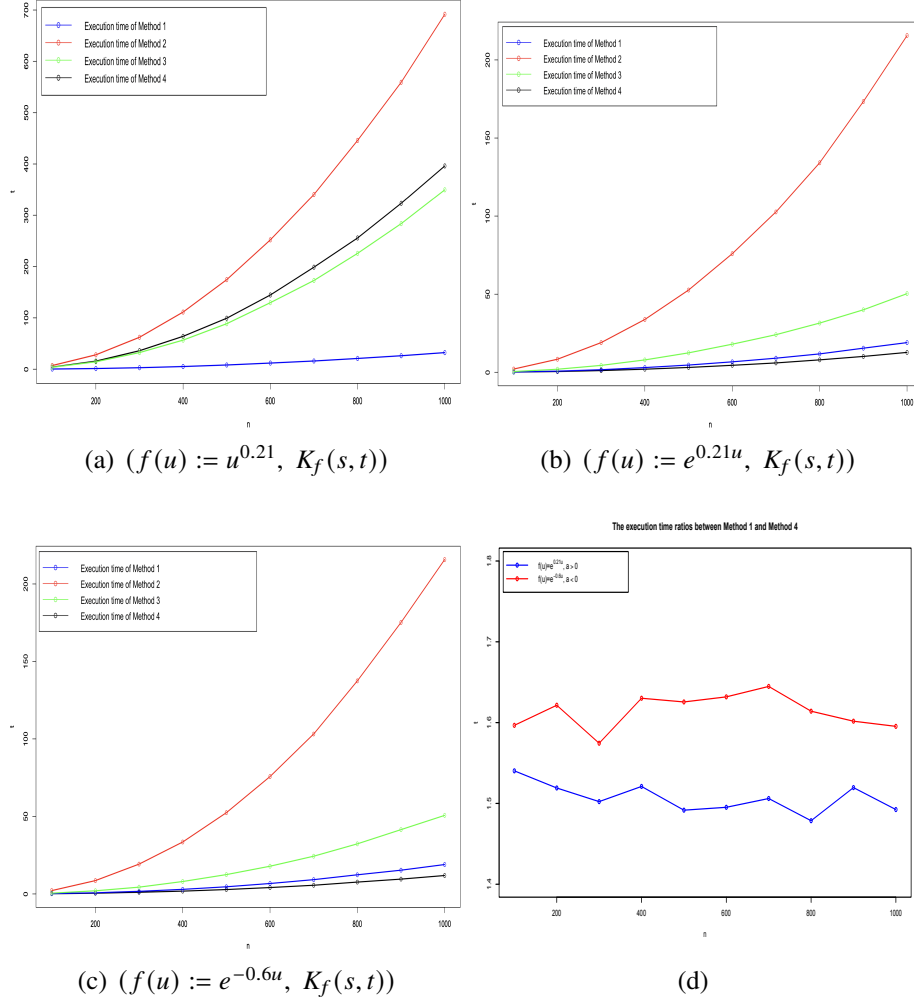


Figure 2: Panel (a), (b), and (c) represent the execution time of calculating the covariance function associated with the process  $\zeta_{t,f}$  over the time vector  $\bar{t}$ . Panel (d) shows the execution time ratios between Method 1 and Method 4 for Panels (b) and (c).

Additionally, analogous studies were conducted considering  $\Delta_i \neq \Delta_j$  for  $i, j = 1, \dots, n$ ,  $i \neq j$ . Specifically,  $t_i$  was considered as the order statistic  $i$  of  $n$  random variables with uniform distribution on  $[0, T]$ . However, the results obtained were similar to those reported in the case  $\Delta_k = \frac{T}{n}$ , for  $k = 1, \dots, n$ .

## 5.2. Inference to simulated data

In this section, we present inferential studies of the finite-dimensional distributions of the process  $\zeta_{t,f,b}$ . Inference was conducted via maximum likelihood estimation using the R software, with the code accessible at <https://github.com/joseramirezgonzalez/Weighted-sfBm>. Let  $T > 0$ ,  $n \in \mathbb{N}$ , and  $\bar{t} = (t_0 := 0, \dots, t_n := T)$  be a partition of the interval  $[0, T]$  into  $n$  blocks, and  $\Delta_k = t_k - t_{k-1}$  for  $k = 1, \dots, n$ . In our analyses, we consider  $\Delta_k = \frac{T}{n}$  for all  $k = 1, \dots, n$  and  $f \in C_1 \cup C_2$ .

A critical value for the parameter vector  $(a, b)$  is given by  $(0, 1)$ . In this case, the finite-dimensional distributions are associated with the covariance function  $K_f(s, t)$  with  $f \equiv 1$ . In our first inferential analysis, we set  $T = 10$ ,  $n = 400$ , and perform a simulation of the finite-dimensional distributions of  $K_f(s, t)$  over the time vector  $\bar{t}$ . We use 90% of the data for inference and the remaining 10% for predictions. We fit the process  $\zeta_{t,f,b}$  over the family of functions  $C_1$  and  $C_2$ . Figure 3 shows the graph of the Likelihood Ratio on family  $C_1$  (panel (a)) and on family  $C_2$  (panel (b)). We obtain the Maximum Likelihood Estimators (MLEs) of the parameters  $(a, b)$ . The MLEs are given by  $(-0.001186, 0.971468)$  for family  $C_1$  and  $(0.003391, 0.976201)$  for family  $C_2$ .

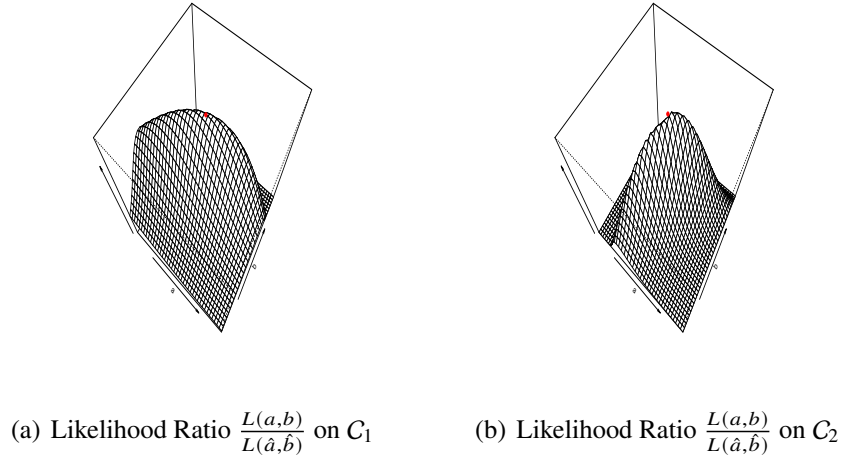


Figure 3: Panel (a): Likelihood ratio function over the family of functions  $C_1$ . Panel (b): Likelihood ratio function over the family of functions  $C_2$ . In the simulations, we consider  $T = 9$ ,  $n = 360$ ,  $\Delta_k = \frac{T}{n}$  and generating with the covariance function of process  $\zeta_{t,f}$ ,  $f \equiv 1$ . Red point is the likelihood ratio function evaluated on the MLEs in both panels.

Confidence intervals at 95% confidence were derived using deviance-based and their distribution, which approximates the chi-square distribution under regularity conditions. For family  $C_1$ , Figure 4 illustrates the profile Likelihood Ratio of parameters  $(a, b)$  and the corresponding confidence intervals. Additionally, the observed symmetry around the MLEs indicates that the Gaussian approximation (GA) can also be utilized to provide confidence intervals. The intervals obtained were  $(-0.091935, 0.093574)$  for  $a$  and  $(0.930338, 1.010467)$  for  $b$ . Hence, the critical value  $(0, 1)$  is considered probable value for inference on the family  $C_1$  based on the simulated data. Furthermore, the model fit yielded an Akaike Information Criterion (AIC) statistic of  $-1546.872$ .

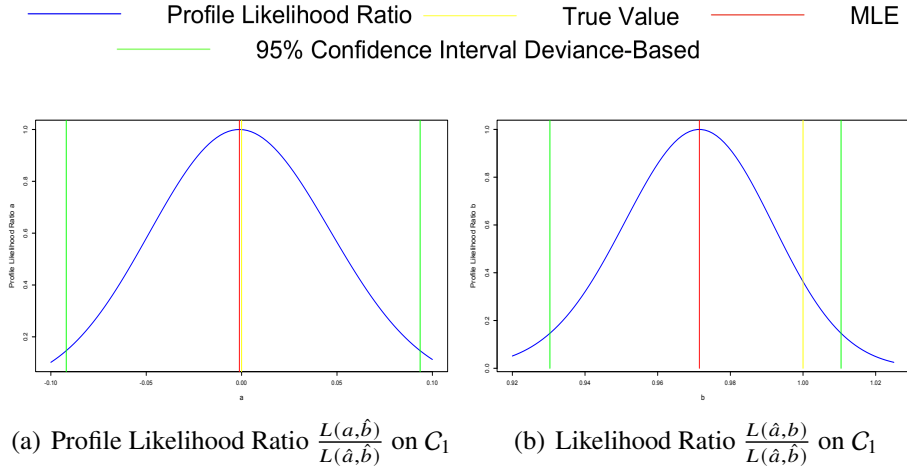


Figure 4: Profile likelihood of parameters for the simulation of  $\zeta_{t,f,b}$  over the family of functions  $C_1$ . In the simulations, we consider  $T = 9$ ,  $n = 360$ ,  $\Delta_k = \frac{T}{n}$  and generating with the covariance function of process  $\zeta_{t,f}$ ,  $f \equiv 1$ .

In the case of family  $C_2$ , Figure 5 displays the profile Likelihood Ratio for parameters  $(a, b)$  along with the 95% confidence intervals using deviance-based. The profile likelihood ratio graph for parameter  $a$  exhibits asymmetry, suggesting that the GA is unsuitable for providing confidence intervals. The derived intervals for  $(a, b)$  were  $(-8.923177e-10, 0.032288)$  and  $(0.934886, 1.01493)$ , respectively. However, assuming  $b = 1$ , panel (b) demonstrates symmetry around the MLE  $(-0.001183)$  for parameter  $a$ , allowing the use of Gaussian approximation to determine confidence intervals. The 95% confidence interval using deviance-based in this scenario is provided by  $(-0.00948, 0.046576)$ . Consequently, the critical value  $(0, 1)$  remains a probable value for inference on the family  $C_2$  based on the

simulated data. Additionally, the AIC is given  $-1546.886$ .

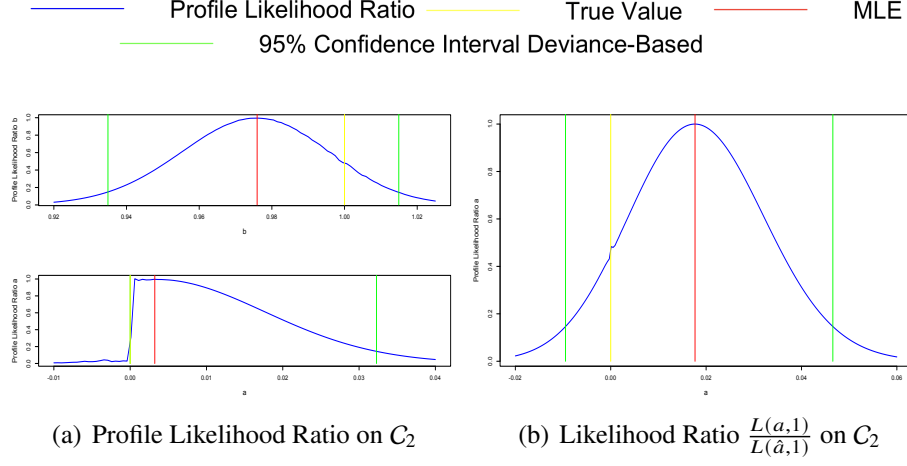
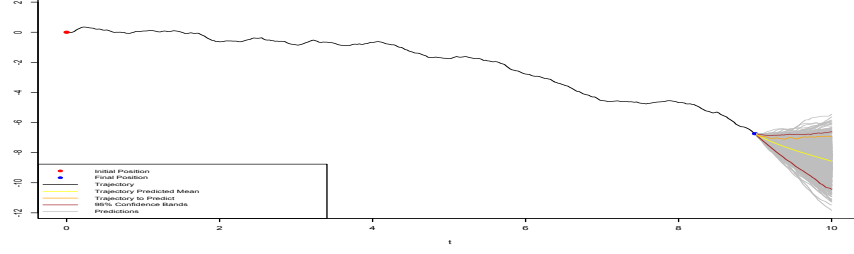


Figure 5: Profile likelihood of parameters for the simulation of  $\zeta_{t,f,b}$  over the family of functions  $C_2$ . In the simulations, we consider  $T = 9$ ,  $n = 360$ ,  $\Delta_k = \frac{T}{n}$  and generating with the covariance function of process  $\zeta_{t,f}$ ,  $f \equiv 1$ .

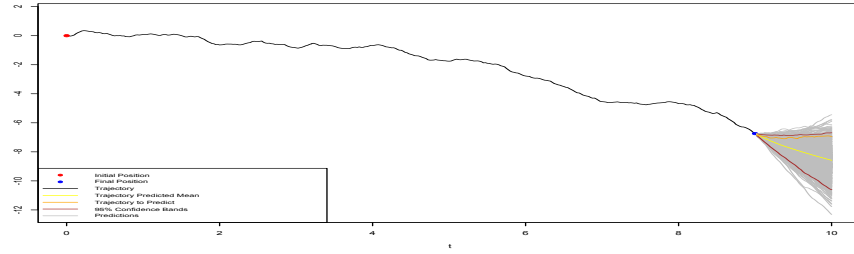
In both cases, the value  $(a, b) = (0, 1)$  is a plausible estimate. Therefore, by performing inference on the finite-dimensional distributions of the covariance function  $K_f(s, t)$  with  $f \equiv 1$ , we obtained an AIC of  $-1548.9$ . This suggests that, according to the AIC criterion, the model  $K_f(s, t)$  with  $f \equiv 1$  provides a better fit for the simulated data. This result demonstrates consistency in the simulated data for the covariance families  $R_{f,b}(s, t)$  over the families  $C_1$  and  $C_2$  as  $(a, b) \rightarrow (0, 1)$  (see Proposition 8 (ii)).

Additionally, we can make trajectory predictions for the next 10% of the simulated data. Figure 6 depicts these predictions. We conducted 1000 simulations and used the predicted mean trajectory (yellow line) for comparison. The results, compared using mean square error with the real data (orange line), yielded a mean square error of 0.930131 under family  $C_1$ , 0.946401 under family  $C_1$ , and 0.909203 under the model  $K_f(s, t)$  with  $f \equiv 1$ . Again, based on mean square error of predictions, the model  $K_f(s, t)$  with  $f \equiv 1$  provides a better fit for the simulated data.

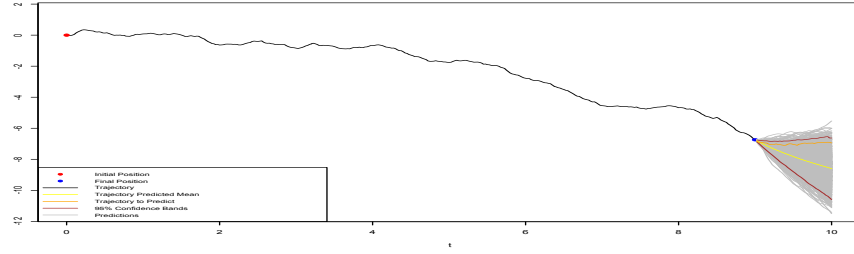




(a) Prediction with  $a = 0, b = 1$



(b) Prediction on  $C_1$  with MLEs



(c) Prediction on  $C_2$  with MLEs

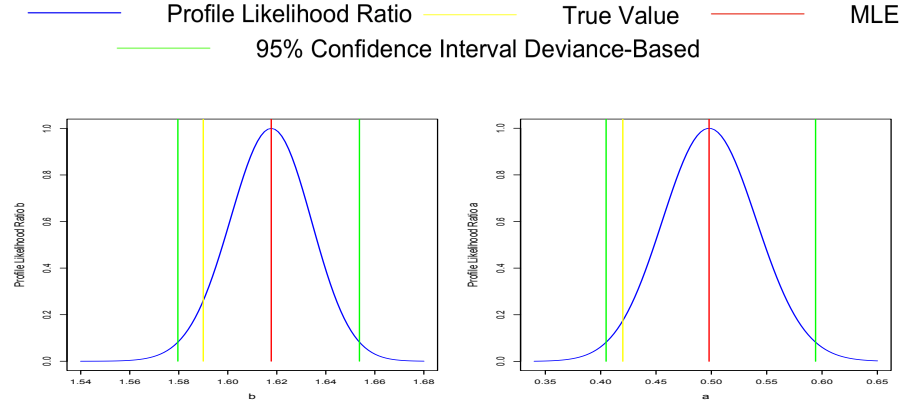
Figure 6: Panel (a): Trajectory prediction for the next 40 steps considering the covariance function of the process  $\zeta_{t,f}$  with  $f \equiv 1$ . Panel (b): Trajectory prediction for the next 40 steps over the family of functions  $C_1$  with parameters estimated by MLEs. Panel (c): Trajectory prediction for the next 40 steps over the family of functions  $C_2$  with parameters estimated by MLEs.

We now present an inferential analysis on simulated data for the process  $\zeta_{t,f,b}$  when  $b \neq 0$ , focusing on the function families  $C_1$  and  $C_2$ . To begin, we consider the scenario where  $f \in C_1$ .

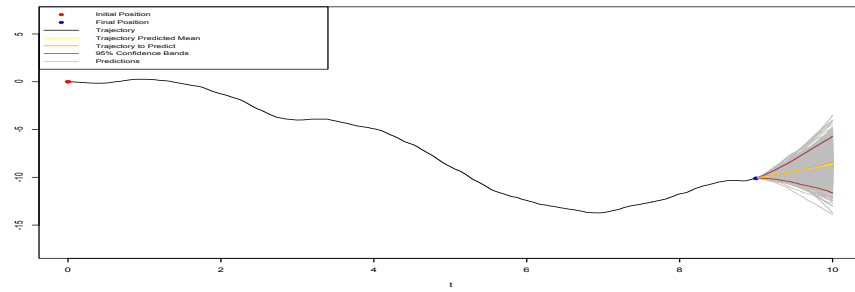
In this simulation, we set  $T = 10, n = 500, b = 1.59, a = 0.42$ , and  $\Delta_k = \frac{T}{n}$ . We simulated the finite-dimensional distributions of  $R_{b,f}(s, t)$  across the time vector  $\bar{t}$ . For our analysis, we used 90% of the data for inference and reserved the remaining

10% for predictions. The process  $\zeta_{t,f,b}$  was fitted using the  $C_1$  function family, yielding MLEs of (0.497943, 1.617743). Additionally, confidence intervals at a 95% level were computed using deviance-based. Figure 7 (panel (a)) shows the profile Likelihood Ratio of parameters  $(a, b)$  along with the corresponding confidence intervals. The symmetry observed in the profile Likelihood Ratio for  $(a, b)$  around the MLEs suggests that the GA is appropriate for providing confidence intervals. The intervals calculated were (0.4049056, 0.5941586) for  $a$  and (1.579637, 1.653722) for  $b$ .

Furthermore, we made trajectory predictions for the subsequent 10% of the simulated data. Figure 7 (panel (b)) displays these predictions. We performed 1000 simulations, using the predicted mean trajectory (yellow line) for comparison. The mean square error, calculated against the real data (orange line), was 0.00543. Since the mean square error of the predictions was in the order of  $10^{-3}$  and the real parameters fall within the 95% confidence intervals, we conclude that inference through likelihood on simulated data is reliable.



(a) Profile Likelihood Ratio parameters  $a$  and  $b$

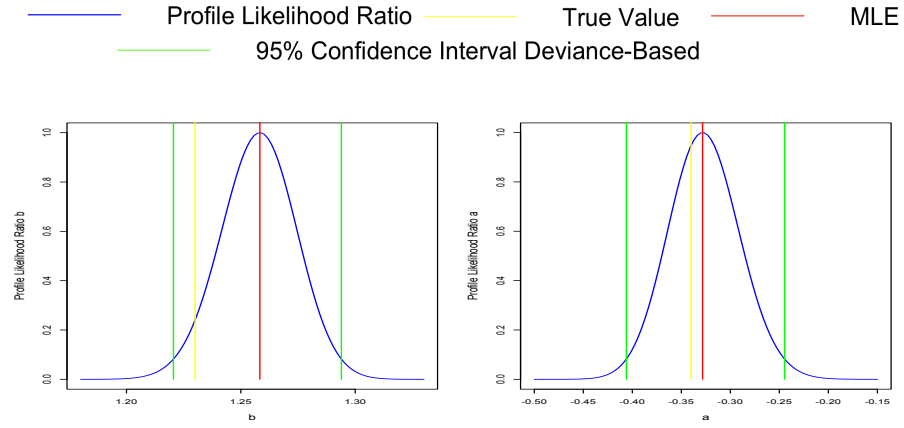


(b) Prediction on  $C_1$  with MLEs

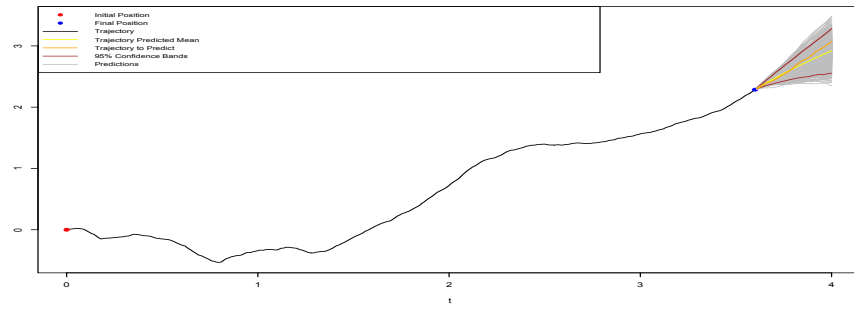
Figure 7: Panel (a): Profile likelihood of parameters for the simulation of  $\zeta_{t,f,b}$  over the family of functions  $C_1$ . In the simulations, we consider  $T = 9$ ,  $n = 450$ ,  $b = 1.59$ ,  $f(u) = u^{0.42}$ , and  $\Delta_k = \frac{T}{n}$ . Panel (b): Trajectory prediction for the next 50 steps over family of functions  $C_1$  with parameters the MLEs.

Finally, we investigate the case where  $f \in C_2$ . For this simulation, we chose  $T = 4$ ,  $n = 400$ ,  $b = 1.23$ ,  $a = -0.34$ ,  $\Delta_k = \frac{T}{n}$ . We conducted a simulation of the finite-dimensional distributions of  $R_{b,f}(s, t)$  over the time vector  $\bar{t}$ . Once again, 90% of the data was utilized for inference, with the remaining 10% set aside for predictions. The process  $\zeta_{t,f,b}$  was fitted using the  $C_2$  function family, resulting in MLEs of  $(-0.3283066, 1.258315)$ . Confidence intervals at a 95% confidence level were derived using deviance-based. Figure 8 (panel (a)) illustrates the profile Likelihood Ratio of parameters  $(a, b)$  and the corresponding confidence intervals. The symmetry in the profile Likelihood Ratio for  $(a, b)$  around the MLEs indicates that the GA can be used to obtain confidence intervals. The intervals obtained were  $(-0.4060894, -0.244653)$  for  $a$  and  $(1.220527, 1.293951)$  for  $b$ .

Additionally, we predicted trajectories for the next 10% of the simulated data. Figure 8 (panel (b)) presents these predictions. We carried out 1000 simulations and compared the predicted mean trajectory (yellow line) with the real data (orange line). The results showed a mean square error of 0.004405. Given that the mean square error of the predictions was of the order  $10^{-3}$  and the true parameters fall within the 95% confidence intervals. Again, we consider that inference through likelihood on simulated data is reliable.



(a) Profile Likelihood Ratio parameters  $a$  and  $b$



(b) Prediction on  $C_2$  with MLEs

Figure 8: Panel (a): Profile likelihood of parameters for the simulation of  $\zeta_{t,f,b}$  over the family of functions  $C_2$ . In the simulations, we consider  $T = 3.6$ ,  $n = 360$ ,  $b = 1.23$ ,  $f(u) = e^{-0.34u}$ , and  $\Delta_k = \frac{T}{n}$ . Panel (b): Trajectory prediction for the next 40 steps over family of functions  $C_2$  with parameters the MLEs.



### 5.3. Auxiliary Figures for the main document

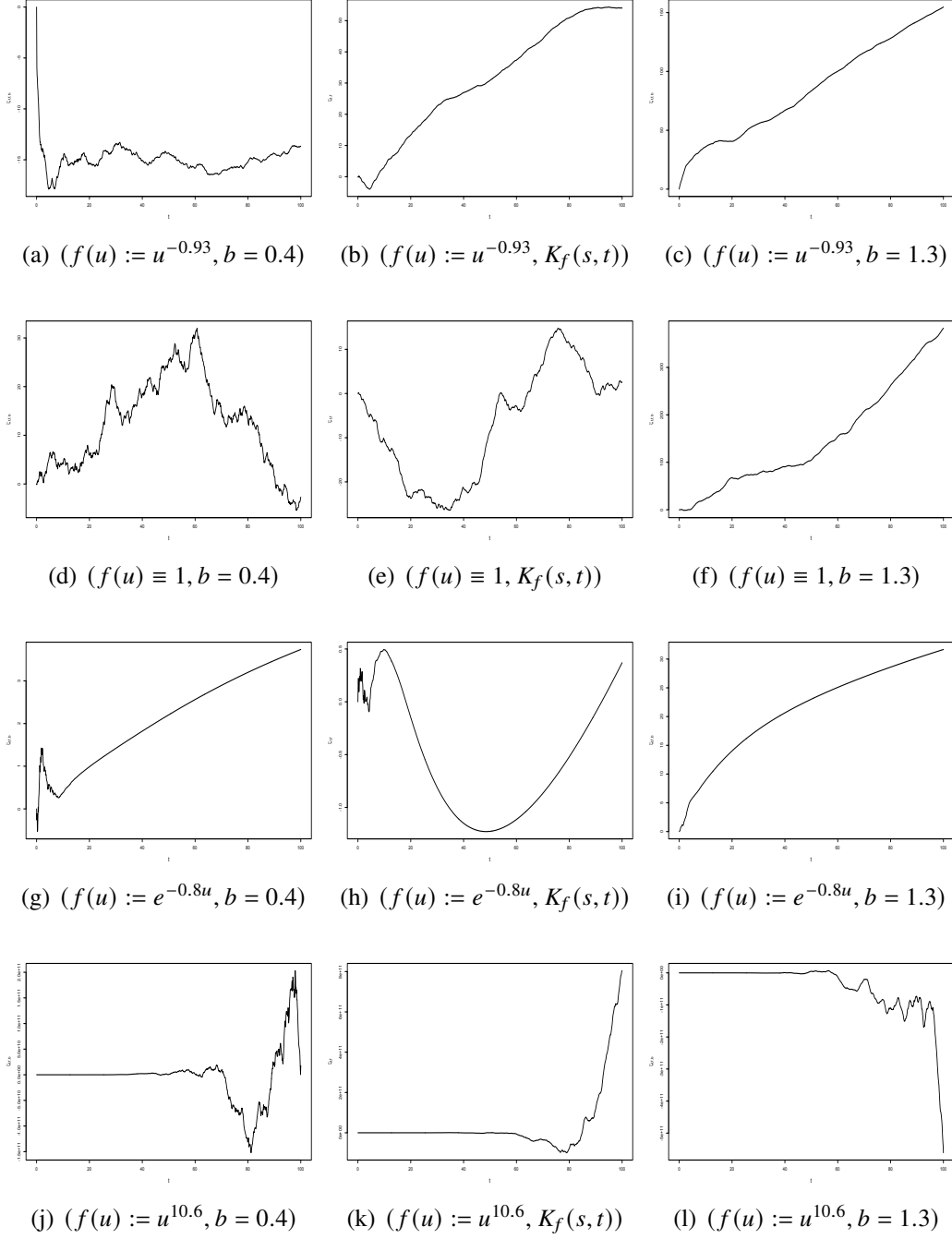
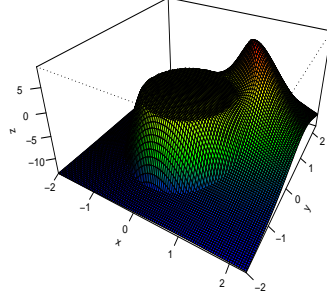
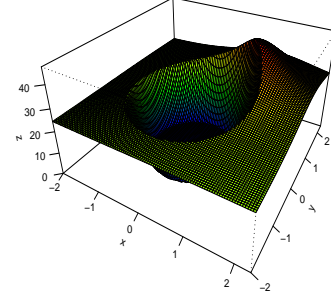


Figure 9: Simulation of  $(\zeta_{t,f,b})_{t \geq 0}$  process. The simulations have been carried out with 1000 equidistant points in the interval  $[0, 100]$ . The initial position is considered to be  $\zeta_{0,f,b} = 0$ .

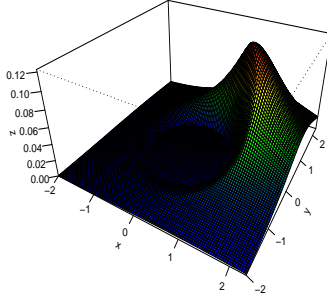
$$K_{M,2,1,4,3}((x,y),p)C_{A,f}((x,y),p)+K_{0,78,g,A,+}((x,y),p), \quad f(u)=||u||^{0.92}, \quad g(u)=e^{-2.4||u||}$$



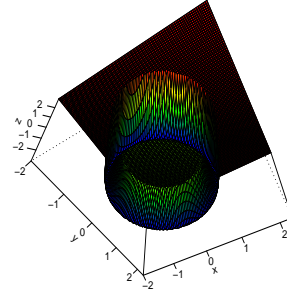
$$K_{M,2,1,4,3}((x,y),p)C_{A,f}((x,y),p)+K_{0,78,g,A,-}((x,y),p), \quad f(u)=||u||^{0.92}, \quad g(u)=e^{-2.4||u||}$$



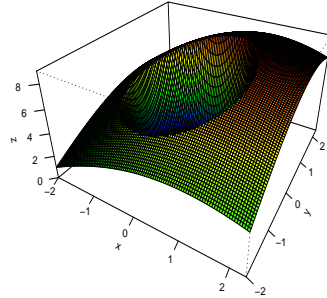
$$K_{M,2,1,4,3}((x,y),p)C_{A,f}((x,y),p), \quad f(u)=e^{-2.4||u||}$$



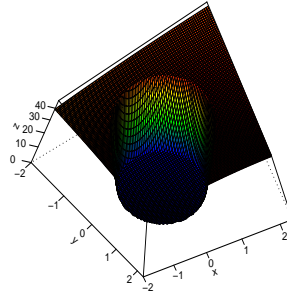
$$K_{0,3,f,A,+}((x,y),p)+K_{0,78,g,A,+}((x,y),p), \quad f(u)=||u||^{0.34}, \quad g(u)=||u||^{0.76}$$



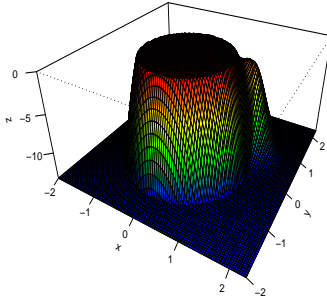
$$K_{RQ,1,2,1,4,3}((x,y),p)C_{A,f}((x,y),p)+K_{0,78,g,A,+}((x,y),p), \quad f(u)=||u||^{0.54}, \quad g(u)=e^{0.1||u||}$$



$$K_{RQ,1,2,1,4,3}((x,y),p)C_{A,f}((x,y),p)+K_{0,78,g,A,-}((x,y),p), \quad f(u)=||u||^{0.54}, \quad g(u)=e^{0.1||u||}$$



$$K_{DE,0.72,8,4}((x,y),p)C_{A,f}((x,y),p)+K_{0,78,g,A,+}((x,y),p), \quad f(u)=||u||^{0.54}, \quad g(u)=e^{0.1||u||}$$



$$K_{P,1,31,1,3,2}((x,y),p)C_{A,f}((x,y),p)+K_{0,78,g,A,+}((x,y),p), \quad f(u)=||u||^{0.54}, \quad g(u)=e^{0.1||u||}$$

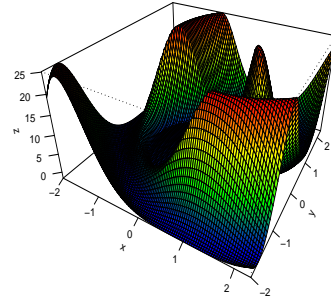


Figure 10: Mixed covariance functions of the form (61), (62), and (64), evaluated at  $((x, y), p)$ . Here,  $p = (2, 2) \in \mathbb{R}^2$  and  $A = B(0, 1) \subset \mathbb{R}^2$  is the unit ball centered at the origin.



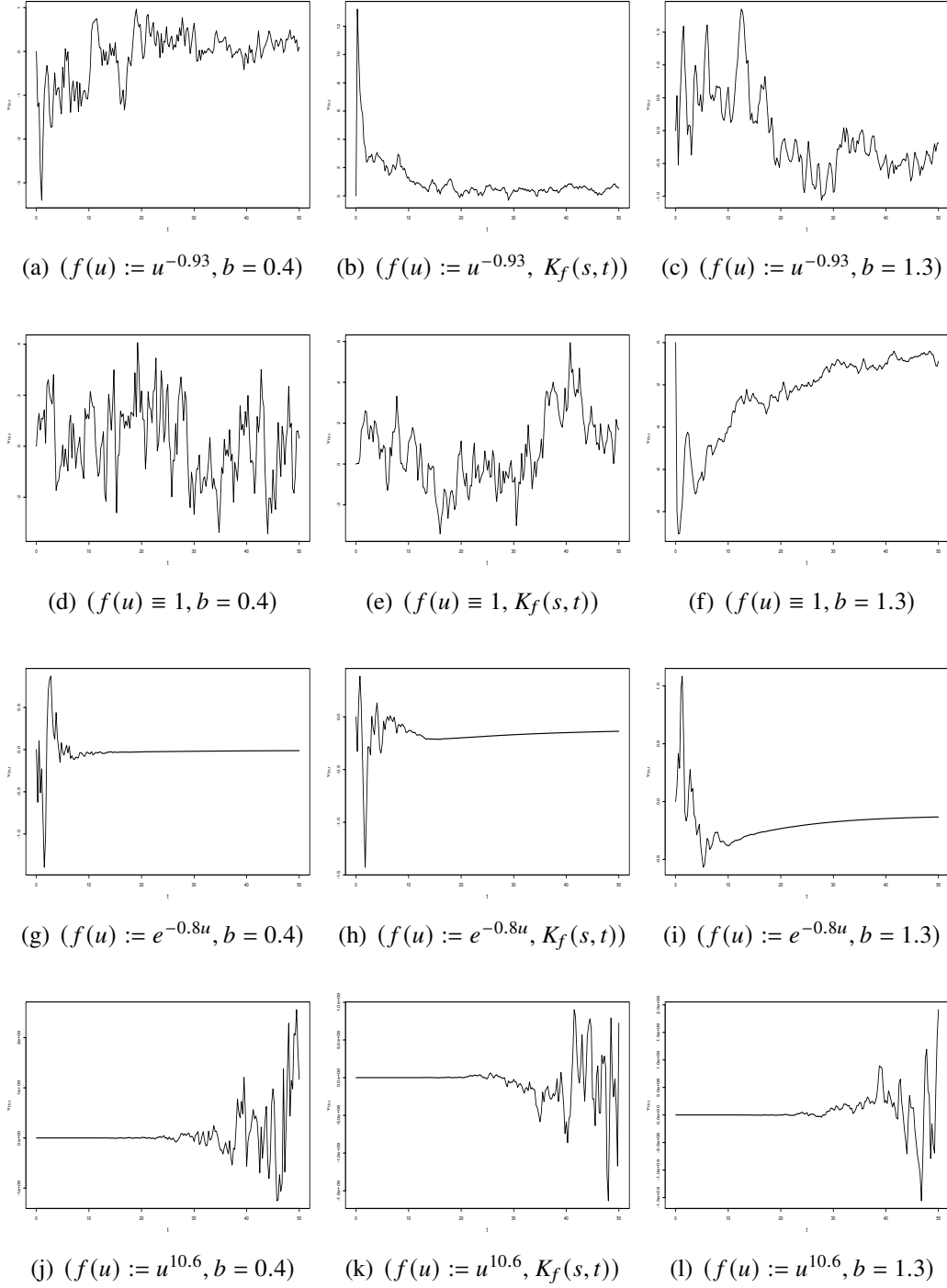


Figure 11: Simulation of  $(V_{f,b,t})_{t \geq 0}$  process. The simulations have been carried out with 200 equidistant points in the interval  $[0, 50]$ . The initial position is considered to be  $V_{f,b,0} = 0, \beta = 3.7$  and  $\sigma = 4.2$ .

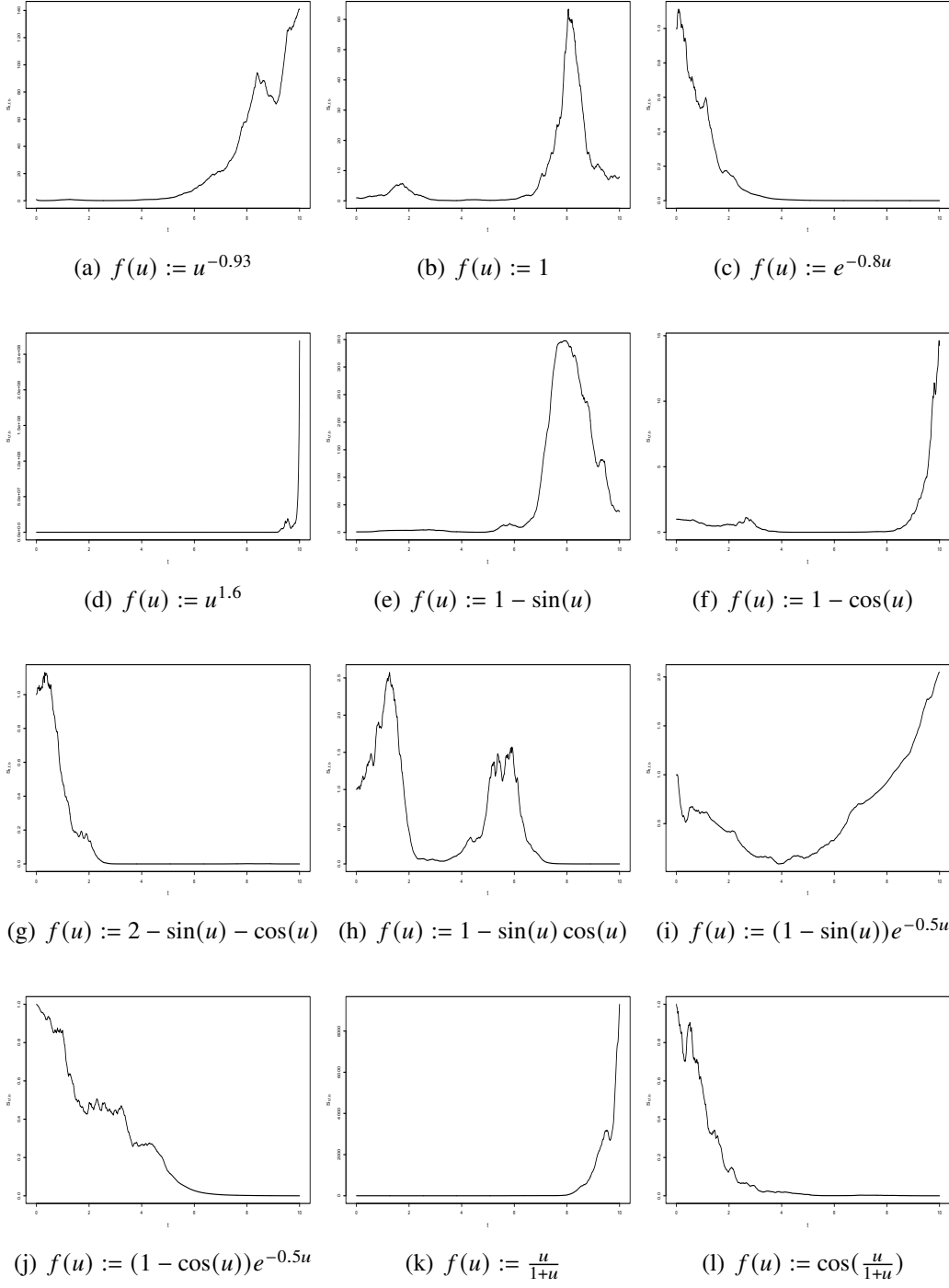


Figure 12: Simulation of  $(S_{t,f,b})_{t \geq 0}$  process. The simulations have been carried out with 1000 equidistant points in the interval  $[0, 10]$ . The initial position is considered to be  $S_{0,f,b} = 1$  and parameters  $b = 1.14$ ,  $\mu = -0.12205$  and  $\sigma = 1.71$ .

## References

- Alsenafi, A., Al-Foraih, M., and Es-Sebaiy, K., *Least squares estimation for non-ergodic weighted fractional Ornstein-Uhlenbeck process of general parameters*, AIMS Mathematics, 6(11), 2021, 12780-12794.
- Amblard, P., Coeurjolly, J.-F., Lavancier, F., and Philippe, A., *Basic properties of the Multivariate Fractional Brownian Motion*, Séminaires et Congrès- SMF, 28, 2013, 65–87.
- Bartoszek, K., Glémin, S., Kaj, I., and Lascoux, M., *Using the Ornstein–Uhlenbeck process to model the evolution of interacting populations*, Journal of Theoretical Biology, 429, 2017, 35–45.
- Bojdecki, T., Gorostiza, L., and Talarczyk, A., *Fractional Brownian Density Process and Its Self-Intersection Local Time of Order  $k$* , Journal of Theoretical Probability, 17, 2004, 717–739.
- Bojdecki, T., Gorostiza, L. G., and Talarczyk, A., *Sub-fractional Brownian motion and its relation to occupation times*, Statist. Probab. Lett., 69(4), 2004, 405–419.
- Bojdecki, T., Gorostiza, L. G., and Talarczyk, A., *Some extensions of fractional Brownian motion and sub-fractional Brownian motion related to particle systems*, Electronic Communications in Probability [electronic only], 12, 2007, 161–172.
- Bojdecki, T., Gorostiza, L., and Talarczyk, A., *Occupation time limits of inhomogeneous Poisson systems of independent particles*, Stochastic Processes and their Applications, 118(1), 2008, 28–52.
- Bojdecki, T., Gorostiza, L., and Talarczyk, A., *Particle systems with quasi-homogeneous initial states and their occupation time fluctuations*, Electronic Communications in Probability, 15, 2010, 191–202.
- Cheridito, P., Kawaguchi, H., and Maejima, M., *Fractional Ornstein-Uhlenbeck processes*, Electronic Journal of Probability, 8, 2003, 1–14.
- Cheung, M. T., Yeung, D., and Lai, A., *On the use of geometric Brownian motion in financial analysis*, In Karmann, A., Mosler, K., Schader, M., and Uebe, G., editors, Operations Research '92, Physica-Verlag HD, Heidelberg, 1993, 541–543.

- Fleischmann, K., Vatutin, V. A., and Wakolbinger, A., *Branching systems with long-lived particles at a critical dimension*, Teor. Veroyatnost. i Primenen., 47(3), 2002, 417–451.
- Genz, Alan, and Malik, Ahmed, *cubature: Adaptive Multivariate Integration over Hypercubes*, R package version 2.0.4, 2023, <https://cran.r-project.org/web/packages/cubature/cubature.pdf>.
- Johnson, D. S., London, J. M., Lea, M.-A., and Durban, J. W., *Continuous-time correlated random walk model for animal telemetry data*, Ecology, 89(5), 2008, 1208–1215.
- Lavancier, F., Philippe, A., and Surgailis, D., *Covariance function of vector self-similar processes*, Statistics & Probability Letters, 79(23), 2009, 2415–2421.
- Liang, Z., Yuen, K. C., and Guo, J., *Optimal proportional reinsurance and investment in a stock market with Ornstein–Uhlenbeck process*, Insurance: Mathematics and Economics, 49(2), 2011, 207–215.
- Litan Yan, Z. W., and Jing, H., *Some path properties of weighted-fractional Brownian motion*, Stochastics, 86(5), 2014, 721–758.
- López-Mimbela, J., Murillo-Salas, A., and Ramírez-González, J. H., *Occupation time fluctuations of an age-dependent critical binary branching particle system*, ALEA, Lat. Am. J. Probab. Math. Stat., 21, 2024.
- Piessens, R., de Doncker-Kapenga, E., Überhuber, C. W., and Kahaner, D., *QUADPACK: A Subroutine Package for Automatic Integration*, Springer-Verlag, 1983.
- Protter, Philip E., *Stochastic Integration and Differential Equations*, Stochastic Modelling and Applied Probability, Vol. 21, Springer, Berlin, Heidelberg, 2nd ed., 2005.
- Ramírez-González, J. H., Chacón-Montalván, E. A., Moraga, P., and Sun, Y., *Multi-Dimensional integral fractional Ornstein-Uhlenbeck process model for animal movement*, 2024, <https://doi.org/10.13140/RG.2.2.21463.07841>.
- Ramírez-González, J. H., Murillo-Salas, A., and Sun, Y., *On a new family of weighted Gaussian processes: an application to bat telemetry data*, 2024, <https://doi.org/10.48550/arXiv.2405.19903>.

- Ramírez-González, J. H., and Sun, Y., *Integral fractional Ornstein-Uhlenbeck process model for animal movement*, 2023, <https://arxiv.org/abs/2312.09900>.
- Russo, Francesco, and Vallois, Pierre, *Stochastic calculus with respect to continuous finite quadratic variation processes*, Stochastics and Stochastic Reports, 70(1-2), 2000, 1–40, DOI: 10.1080/17442500008834244.
- Stojkoski, Viktor, Sandev, Trifce, Basnarkov, Lasko, Kocarev, Ljupco, and Metzler, Ralf, *Generalised geometric brownian motion: Theory and applications to option pricing*, Entropy, 22(12), 2020, 1432, DOI: 10.3390/e22121432.
- Sun, Lin, Chen, Jianxin, and Lu, Xianggang, *Parameter estimation for discretized geometric fractional Brownian motions with applications in Chinese financial markets*, Advances in Continuous and Discrete Models, 2022(1), 2022, 69.
- Sun, X., Yan, L., and Zhang, Q., *The quadratic covariation for a weighted fractional Brownian motion*, Stochastics and Dynamics, 17(04), 2017, 1750029.
- Vatutin, V. A., and Wakolbinger, A., *Branching processes in long-lived particles*, Teor. Veroyatnost. i Primenen., 43(4), 1998, 655–671.
- Wheeden, R. L., and Zygmund, A., *Measure and Integral: An Introduction to Real Analysis*, CRC Press, 1977.
- Xu, F., and Yang, X.-J., *Pricing European Options under a Fuzzy Mixed Weighted Fractional Brownian Motion Model with Jumps*, Fractal and Fractional, 7(12), 2023.